

Aus der Medizinischen Klinik und Poliklinik IV  
der Ludwig-Maximilians-Universität München



**Aldosterone-induced changes in endothelial function:  
The epoxyeicosatrienoic acid pathway in aldosterone excess  
and receptor transactivation by co-stimulation with gluco- and  
mineralocorticoids.**

Dissertation  
zum Erwerb des Doktorgrades der Medizin  
an der Medizinischen Fakultät der  
Ludwig-Maximilians-Universität München

vorgelegt von  
Yao Meng  
aus  
Lin Xia

2022

---

Mit Genehmigung der Medizinischen Fakultät der  
Ludwig-Maximilians-Universität zu München

Erster Gutachter: Professor Dr. med. Martin Reincke

Zweiter Gutachter: Professor Dr. med. Nicole Reisch-Pawlu

Dritter Gutachter: Professor Dr. med. Andreas Schober

Mitbetreuung durch den  
promovierten Mitarbeiter: Dr. med. Holger Schneider

Dekan: Prof. Dr. med. Thomas Gudermann

Tag der mündlichen Prüfung: 24.11.2022

# Table of content

<b>Table of content.....</b>	<b>3</b>
<b>Zusammenfassung (Deutsch):.....</b>	<b>5</b>
<b>Abstract (English): .....</b>	<b>7</b>
<b>List of figures.....</b>	<b>8</b>
<b>List of tables .....</b>	<b>9</b>
<b>List of abbreviations .....</b>	<b>11</b>
<b>1. Introduction .....</b>	<b>13</b>
1.1 Primary aldosteronism (PA) .....	13
1.1.1 Epidemiology and clinical diagnosis .....	13
1.1.2 Organ damage in PA .....	14
1.2 Endothelial factors .....	15
1.2.1 Overview .....	15
1.2.2 Epoxyeicosatrienoic acids (EETs) .....	16
1.2.3 Intersection of EETs and primary aldosteronism .....	18
1.3 Corticosteroid receptor transactivation .....	19
1.4 Study aims .....	22
<b>2. Material and Methods .....</b>	<b>23</b>
2.1 Cell culture and stimulation.....	23
2.1.1 List of materials for cell culture .....	23
2.2 RNA extraction, reverse transcription and qPCR .....	24
2.2.1 List of materials for RNA extraction, reverse transcription and qPCR .....	24
2.2.2 RNA extraction.....	24
2.2.3 Reverse transcription .....	25
2.2.4 Quantitative real-time PCR (qPCR) .....	25
2.3 Fluo4-based calcium imaging .....	27
2.3.1 Materials for calcium imaging .....	27
2.3.2 Calcium imaging .....	27
2.4 Stimulation of endothelial EET release.....	28
2.5 Quantification of EETs and DHETs in endothelial supernatant .....	28
2.5.1 HPLC-MS/MS.....	28
2.5.2 Validation procedure .....	28
2.6 Determination of steroids in endothelial culture supernatants .....	29
2.7 Immunofluorescence of endothelial cells .....	30
2.7.1 Materials for immunofluorescence .....	30
2.8 Statistics.....	31
<b>3. Results .....</b>	<b>32</b>
3.1 Part A: Endothelial eicosanoids in aldosterone excess .....	32
3.1.1 EET-related mRNA expression data in endothelial cells .....	32
3.1.2 Quantification of stimulated EET release from endothelial cells.....	36

3.2	Part B: Cross-talk of endothelial glucocorticoid and mineralocorticoid receptors in aldosterone excess .....	40
3.2.1	Expression levels of endothelial 11 $\beta$ -hydroxysteroid dehydrogenases and their activities .....	40
3.2.2	MR and GR marker gene transcription and interaction .....	43
3.2.3	Semiquantitative parallel analysis of MR and GR activation by immunofluorescence ....	45
<b>4.</b>	<b>Discussion .....</b>	<b>48</b>
4.1	Part A .....	48
4.1.1	Gene expression levels.....	48
4.1.2	Calcium response in endothelial cells.....	50
4.1.3	Stimulated EET release by endothelial cells.....	51
4.2	Part B .....	52
4.2.1	Expression levels of endothelial 11 $\beta$ -hydroxysteroid dehydrogenases and their activities .....	52
4.2.2	MR and GR marker gene transcription and interaction .....	54
4.2.3	Semiquantitative parallel analysis of MR and GR activation by immunofluorescence ....	56
<b>References .....</b>	<b>58</b>	
<b>Acknowledgements.....</b>	<b>66</b>	
<b>Affidavit .....</b>	<b>67</b>	
<b>List of publications .....</b>	<b>68</b>	

## Zusammenfassung (Deutsch):

Patienten mit primärem Hyperaldosteronismus weisen regelhaft ein Übermaß an kardiovaskulären Begleiterkrankungen auf, die nicht durch das Ausmaß der arteriellen Hypertonie erklärt werden. Diese Begleiterkrankungen haben dieselben Ätiologien wie die Folgeerkrankungen der Arteriosklerose, für die wiederum die endotheliale Dysfunktion den ersten pathogenetischen Schritt darstellt. Endothelzellen sind durch ein breites Repertoire an Signalwegen charakterisiert, über die sie vaskuläre glatte Muskelzellen relaxieren und die Gefäßhomöostase aufrechterhalten. Einen dieser Signalwege stellt der Epoxyeicosatriensäure (EET)-Signalweg dar, welcher zur übergeordneten Signalwegfamilie des endothelium-derived hyperpolarizing factor (EDHF) zählt. Derzeit ist wenig bekannt über die Frage, ob der primäre Hyperaldosteronismus die EET-Freisetzung aus Endothelzellen beeinträchtigt. Erkenntniszugewinne auf diesem Gebiet könnten sich translational in therapeutischen Ansätzen niederschlagen, in denen der EET-Abbau gehemmt wird um letztlich die im Rahmen des Hyperaldosteronismus auftretenden kardiovaskulären Begleiterkrankungen zu behandeln.

Endotheliale Mineralokortikoidrezeptoren sind nicht nur gegenüber Aldosteron exponiert, sondern auch gegenüber den in viel höheren Konzentrationen zirkulierenden Glukokortikoiden. Mineralokortikoidrezeptoren werden durch 11- $\beta$ -HSD (Hydroxysteroiddehydrogenase) Typ 2 vor Glukokortikoiden in einer zelltypspezifischen Weise geschützt. Es bestehen noch deutliche Wissenslücken in Bezug auf die Rolle dieses Glukokortikoidinaktivierungssystems in Endothelzellen und dessen Rolle bei Mineralokortikoidexzess.

Die Ziele dieses Projektes waren daher (A), eine potentielle Beeinträchtigung endothelialer EETs im Kontext einer aldosteroninduzierten endothelialen Dysfunktion zu untersuchen und (B) das Vorhandensein und das Ausmaß einer Transaktivierung von Gluko- und Mineralokortikoidrezeptoren in Endothelzellen zu bestimmen.

Es konnte gezeigt werden, dass Endothelzellen, die einem Aldosteronexzess ausgesetzt waren, ihre ursprünglichen Expressionslevel von Enzymen erhalten, welche für die Synthese und den Abbau von EETs wichtig sind. Auf der anderen Seite führte Aldosteron zu einer vermehrten Expression eines mesenchymalen Markergens und beeinträchtigte den endothelialen Kalziumeinstrom auf Acetylcholin, was als Bestätigung der biologischen Aktivität der verwendeten Steroidkonzentrationen gewertet wurde.

Trotz dieser fundamentalen Änderungen in der Endothelphysiologie war die stimulierte EET-Freisetzung in das Endothelmedium unbeeinträchtigt, was für einen intakten endothelialen EET-Signalweg bei primärem Hyperaldosteronismus spricht. Eine Hemmung des EET-Abbaus könnte daher eine sinnvolle therapeutische Option darstellen, um vaskuläre Erkrankungen bei primärem Hyperaldosteronismus zu behandeln, da die EET-Synthese ungestört ist.

In Bezug auf Ziel (B) zeigten sich vernachlässigbar geringe Expressionslevel von 11- $\beta$ -HSD Typ 1 und Typ 2 in Endothelzellen. Diese Daten konnten funktionell bestätigt werden durch Messungen von Cortison und Cortisol im Zellkulturüberstand. Verschiedene (erhöhte) Konzentrationen von Aldosteron hatten keine Auswirkung auf die Expression beider 11- $\beta$ -HSD Typen. Traditionelle Marker von Transkriptionsaktivität für den Mineralokortikoid- wie auch den Glukokortikoidrezeptor konnten sich jedoch für die Anwendung an Endothelzellen nicht bewähren, da sie auf Stimulation mit Aldosteron und Cortisol keine wesentlichen Expressionsänderungen zeigten. Es konnte ein semiquantitativer, immunfluoreszenzbasierter Kernlokalisierungs-Assay für Steroidrezeptoren etabliert werden. Dieser zeigte, dass Aldosteron in einer mineralokortikoidrezeptorvermittelten Weise die Lokalisierung von Glukokortikoidrezeptoren im Kern hemmte. Auf

Basis dieses neuartigen Befundes kann vermutet werden, dass Mineralokortikoide unter bestimmten Umständen glukokortikoide Wirkung antagonisieren könnten und unterstreicht die komplexe Interaktion beider Steroide. Der entwickelte Assay soll in künftigen Untersuchungen an Geweben von Patienten mit singulärer oder kombinierter Übersekretion von Mineralo- und Glukokortikoiden zum Einsatz kommen, um die endotheliale Steroid-Interaktion nach in vivo-Exposition näher zu untersuchen.

## **Abstract (English):**

Patients with primary aldosteronism (PA) are characterized by an excess of cardiovascular morbidities independent of the degree of associated arterial hypertension. These comorbidities share the same etiology as the sequelae of atherosclerosis of which endothelial dysfunction is considered to be the initiating step. Endothelial cells feature a variety of pathways to relax vascular smooth muscle and maintain a healthy vascular homeostasis, one of the pathways being the epoxyeicosatrienoic acid (EET) pathway as a component of the endothelium-derived hyperpolarizing factor (EDHF) family. At present, little is known about whether primary aldosteronism affects EET release from endothelial cells. Knowledge about the EET pathway functional integrity could translate to therapeutic applications targeting EET breakdown to ultimately target the cardiovascular comorbidities observed in PA.

Endothelial mineralocorticoid receptors are exposed not only to aldosterone but also to circulating glucocorticoids at much higher concentrations. 11- $\beta$ -HSD (hydroxysteroid dehydrogenase) type 2 protects mineralocorticoid receptors from glucocorticoids in a cell-type specific manner. Significant knowledge gaps still exist with regard to the role of this glucocorticoid inactivation system in endothelial cells and its role in mineralocorticoid excess.

The aims of this project were (A) to investigate a potential impairment of endothelium-derived vasoactive EETs in a context of aldosterone-induced endothelial dysfunction and (B) to determine the existence and the degree of endothelial gluco- and mineralocorticoid receptor transactivation.

It could be shown that endothelial cells exposed to aldosterone excess retain their original expression levels of enzymes critical for the synthesis and degradation of EETs. On the other hand, aldosterone increased expression levels of a mesenchymal marker gene and impaired calcium response to stimulation by acetylcholine, thereby underpinning the biological activity of the steroid concentrations which were used. Despite these broad changes in endothelial physiology, stimulated secretion of EETs into the endothelial supernatant was unchanged in conditions of aldosterone excess, arguing for an undisturbed endothelial EET pathway in primary aldosteronism. Because of the seemingly unimpaired EET synthesis, inhibition of EET breakdown may therefore be a reasonable therapeutic option in treating vascular disease in primary aldosteronism.

With respect to aim (B), qPCR revealed negligible expression levels of both 11- $\beta$ -HSD type 1 or 11- $\beta$ -HSD type 2. These data could be corroborated functionally by measurements of cortisone and cortisol in the supernatants. Aldosterone at various concentrations did not modulate the expression or activity of both 11- $\beta$ -HSD enzymes. Traditional markers of transcriptional activity of mineralocorticoid and glucocorticoid receptors turned out to be not useful for endothelial cells, since they could not be shown to be affected by stimulation with cortisol and aldosterone. A semiquantitative, immunofluorescence-based nuclear localization assay of steroid receptors as global readout of activity was established. This assay revealed that aldosterone antagonized nuclear translocation of glucocorticoid receptors in a mineralocorticoid receptor-dependent manner. This novel finding suggests that under certain circumstances mineralocorticoids might antagonize glucocorticoids and highlights the complex interaction between both corticosteroids. Future studies will apply the developed assay to tissues derived from patients harboring single and combined excessive secretion of gluco- and mineralocorticoids to further investigate steroid interactions in endothelial cells following *in vivo* exposure.

## List of figures

**Figure 1.** Overview of selected factors secreted by endothelial cells in response to either mechanical (shear stress) or chemical (acetylcholine, bradykinin) stimuli and their action on underlying smooth muscle cells. All stimuli converge on an elevation in endothelial cytosolic calcium (\*). This then mediates activation of nitric oxide synthase (NOS) which generates NO which in turn elevates smooth muscle cGMP. Calcium is also critical to activate superoxide dismutase (SOD) for the generation of H<sub>2</sub>O<sub>2</sub>, and for the activation of CYP epoxygenases for the synthesis of EETs. A lot of endothelial factors mediate smooth muscle relaxation by activating B<sub>KCa</sub> channels (NO, H<sub>2</sub>O<sub>2</sub>, EETs), others act by direct passage of hyperpolarizing currents (myoendothelial junctions, MEJ) and by activating sodium-potassium ATPase and inward rectifying potassium channels (Kir2.1) (release of K<sup>+</sup>). The mechanism of EETs is still not fully resolved and may either involve a direct action on smooth muscle or an auto-stimulation of endothelial cells with subsequent release of hyperpolarizing factors or passage of hyperpolarizing currents to smooth muscle via MEJ. Endothelium-derived vasodilators not only acutely dilate vessels but also stabilize the normal smooth muscle contractile phenotype, thereby preventing a pro-atherogenic synthetic phenotype switch. .....16

**Figure 2.** Generation and degradation of EETs in vascular cells. Upon release of arachidonic acid, EETs (green box) are generated by CYP epoxygenases in endothelial cells. They are inactivated to DHETs (red box) by microsomal epoxide hydrolase (mEH, EPHX1) and soluble epoxide hydrolase (sEH, EPHX2) expressed in both endothelial and smooth muscle cells. EPHX2 can be inhibited pharmacologically by GSK 2256294 (GSK). .....18

**Figure 3.** Tissue selective MR activation is controlled by cell type-specific expression levels of 11-β-HSD type 1 and type 2. 11-β-HSD type 2 catalyzes cortisol inactivation to cortisone while 11-β-HSD type 1 catalyzes the reverse reaction. Cortisol and aldosterone bind to mineralocorticoid receptors (MR) while cortisone does not. MR-steroid complexed then translocate to the nucleus where they bind to glucocorticoid response elements (GRE) of accessible DNA. Figure modified according to Hudson, Youn and Ortlund, 2014. .....21

**Figure 4.** α-actin (ACTA2) mRNA expression in human coronary artery endothelial cells as a marker of endothelial to mesenchymal transition in response to 48 hours of stimulation with the indicated treatments. Aldo, aldosterone, Ep, eplerenone; n=3-6 independent replicates per treatment; \*: p<0.05, \*\*p<0.01, t-test. .....32

**Figure 5.** Gene expression patterns of CYP epoxygenases required for EET synthesis (**A**, CYP2C8; **B**, CYP2J2) and expression patterns of epoxide hydrolases required for inactivation of EETs (**C**, EPHX1 [mEH]; **D**, EPHX2 [sEH]) in human coronary artery endothelial cells in response to 48 hours of stimulation with the indicated treatments. Aldo, aldosterone, Ep, eplerenone; n=3 independent replicates per treatment. .....34

**Figure 6.** Example tracings of Fluo4 calcium signals in endothelial cells over time in response to the different acetylcholine concentrations used. ACh, acetylcholine; RFU, relative fluorescence units (F/F<sub>0</sub>). .....35

**Figure 7.** Calcium concentration-response curve for acetylcholine as determined by Fluo4 fluorescence in EC cultured for 48 hours in the presence of the indicated treatments. Aldo, 1 μM aldosterone; Ep, 2 μM eplerenone; N=6-11 measurements of at least 3 independent experiments per group and concentration. \*\*, p<0.01 (Cortisol vs. Cortisol +Aldo and Cortisol vs. DMSO at 10 μM acetylcholine). 2-Way ANOVA, Dunnett. .....35

**Figure 8.** Overview of all EETs and DHETs and derived parameters in supernatants from endothelial cells after indicated treatments. Cells acutely stimulated with 1 μM ACh are represented by box plots in **light colors**. Cells acutely stimulated with 100 μM ACh are represented by **dark colors**. To compare acetylcholine concentration effects, cells who underwent identical culture conditions prior to stimulation but

were simulated with different ACh concentrations are superimposed. Overlapping box plots indicate no effect of ACh concentration, separated box plots indicate ACh concentration-dependent effect. ACh, acetylcholine; Aldo, aldosterone; Ep, eplerenone; GSK, GSK2256294. *: p<0.05, **p<0.01, ***p<0.001 (ACh 1 $\mu$ M vs. 100 $\mu$ M), 1-way ANOVA, Šídák.....	39
<b>Figure 9.</b> Relative mRNA expression levels of HSD11B1 (left) and HSD11B2 (left) in endothelial cells after 48 hours of indicated treatment. Shown are means of three independent replicates. ....	40
<b>Figure 10.</b> Steroids in supernatants of endothelial cells after 48 hours of treatment. <b>A</b> , cortisol; **** p<0.0001 versus Hydrocortisone + DMSO, 1-Way ANOVA, Dunnett. <b>B</b> , cortisone; *** p<0.001, ****p<0.0001 versus Hydrocortisone + DMSO, 1-Way ANOVA, Dunnett. <b>C</b> , cortisol/cortisone ratio; ** p<0.01, ***p<0.001 versus Hydrocortisone + DMSO, 1-Way ANOVA, Dunnett.; <b>D</b> , aldosterone; **p<0.01, Aldo 100 nM + hydrocortisone versus Aldo100 nM + hydrocortisone + eplerenone, 1-Way ANOVA, Sidak. Red dotted line indicates intended aldosterone concentrations to delineate possible effects of eplerenone versus the unantagonized stimulation. All concentrations in nmol/L. n=3-9 independent replicates per treatment. Values as means $\pm$ SEM. ....	43
<b>Figure 11.</b> Expression levels of the GR marker gene FKBP5 (left) and the MR marker gene SCNN1A (right) in response to isolated and combined mineralocorticoid and glucocorticoid application and respective antagonization. N=3-6 independent replicates per treatment. *p<0.05 versus DMSO treatment, 1-Way-ANOVA, Dunnett's. ....	44
<b>Figure 12.</b> Aldosterone concentration-response curve. Left, GR marker gene FKBP5, middle, MR marker gene SCNN1A, right, putative MR marker gene NFKBIA. Values as means $\pm$ SEM. n=3 independent replicates per treatment. 1-Way ANOVA, Dunnett. *p<0.05 versus Aldo 1 nM + cortisol, **, p<0.01 versus Aldo 1 nM + cortisol. ....	44
<b>Figure 13.</b> <b>A</b> , original immunofluorescence images of four different treatment conditions (DMSO, 140 nM cortisol, 140 nM cortisol + 1 nM aldosterone, 140 nM cortisol + 1 nM aldosterone + 2 $\mu$ M eplerenone with nuclear DAPI signal in blue (left column), MR signal in red (middle column) and GR signal in green (right column). Images were not digitally manipulated and are presented as they were recorded. White scale bars 50 $\mu$ m. <b>B</b> , summary of mean grey values for MR and GR in the nuclear ROIs. n= 9 different analyses from 3 independent replicates per treatment group. *p<0.05, 1-Way ANOVA, Dunnett. DAPI, 4',6-diamidino-2-phenylindole. MR, mineralocorticoid receptor, GR, glucocorticoid receptor. ....	46

## List of tables

<b>Table 1:</b> Cardiovascular damage in patients with primary aldosteronism (PA) compared to patients with essential hypertension (EH). Patients were matched for age, sex and blood pressure. Data according to Ohno <i>et al.</i> , 2018.....	14
<b>Table 2.</b> Genes of interest and corresponding Taqman probes used in the qPCR experiments .....	26
<b>Table 3.</b> MS transitions and parameter settings for the determination of EETs.....	29
<b>Table 4.</b> Q1 fragment mass (Q1 mass), Q3 fragment mass (Q3 mass), dwell time, collision energy (CE) and retention time (RT) for the mass spectrometric detection of quantifier, qualifier and internal standard transitions of aldosterone, cortisol and cortisone. ....	30
<b>Table 5.</b> EET and DHET in EC supernatant after stimulation with 1 $\mu$ M acetylcholine. Values as mean (SEM). Aldo, aldosterone 1 nM; DHET, dihydroxyeicosatrienoic acid; EC, endothelial cells; EET, epoxyeicosatrienoic acid; Ep, eplerenone 2 $\mu$ M;	

---

GSK, GSK 2256294 3.3 nM. *, p<0.05 vs. cortisol; 1-Way ANOVA, Dunnett. §p<0.05, §§p<0.01, §§§p<0.001 against the same treatment during culture and stimulation with <b>100 <math>\mu</math>M</b> ACh, 1-way ANOVA, Šídák. ....	37
<b>Table 6.</b> EET and DHET in EC supernatant after stimulation with <b>100 <math>\mu</math>M</b> acetylcholine. Values as mean (SEM). Aldo, aldosterone 1 nM; DHET, dihydroxyeicosatrienoic acid; EC, endothelial cells; EET, epoxyeicosatrienoic acid; Ep, eplerenone 2 $\mu$ M; GSK, GSK 2256294 3.3 nM. 1-Way ANOVA, Dunnett. §p<0.05, §§p<0.01, §§§p<0.001 against the same treatment during culture and stimulation with <b>1 <math>\mu</math>M</b> ACh, 1-way ANOVA, Šídák. ....	38
<b>Table 7.</b> Concentrations of indicated steroids as determined by LC-MS/MS in endothelial cell culture supernatants harvested after 48 hours of specific treatment. Values as mean (SEM). Aldo, aldosterone; Ep, eplerenone. Number of replicates is provided in parentheses in the treatment column. ....	42

## List of abbreviations

14,15-EET	14,15-epoxyeicosatrienoic acid
11- $\beta$ -HSD	11- $\beta$ -hydroxysteroid-dehydrogenase
ACTA2	Gene code for smooth muscular $\alpha$ -actin
Aldo	Aldosterone
BCA	Bicinchoninc acid
BSA	bovine serum albumin
[Ca <sup>2+</sup> ] <sub>i</sub>	intracellular calcium concentration
cDNA	complementary DNA, DNA, reverse transcribed from RNA
CT	Cycle Threshold
Ctrl	Control
DHET	Dihydroxyeicosatrienoic acid
DMSO	Dimethyl sulfoxide
DPBS	Dulbecco's phosphate-buffered saline
EBM	endothelial cell basal medium
EGM	endothelial cell growth medium
EET	Epoxyeicosatrienoic acid
EDHF	endothelium-derived hyperpolarizing factor
eNaC	epithelial sodium channel
Ep	Eplerenone
F	Hydrocortisone
GR	Glucocorticoid receptor
GSK	GSK 2256294
h	Hour
HEPES	2-(4-(2-hydroxyethyl)-1-piperazinyl)-ethanesulfonic acid
HSD11B1	gene code for 11- $\beta$ - hydroxysteroid dehydrogenase (HSD) type 1
HSD11B2	gene code for 11- $\beta$ - hydroxysteroid dehydrogenase (HSD) type 2
IP <sub>3</sub>	Inositol trisphosphate
mEH	Microsomal epoxide hydrolase
MR	Mineralocorticoid receptor
n	number of experiments
RT-qPCR	Reverse transcription quantitative polymerase chain reaction

PA	Primary aldosteronism
TBS-T	Tris-buffered saline with Tween20
RyR	Ryanodine receptor
rpm	rounds per minute
sEH	soluble epoxide hydrolase
SEM	standard error of the mean

# 1. Introduction

## 1.1 Primary aldosteronism (PA)

### 1.1.1 Epidemiology and clinical diagnosis

Primary aldosteronism (PA) is the most frequent form of endocrine hypertension with prevalence estimates ranging from 5 to 20 % of patients with arterial hypertension, depending on the setting (primary care versus tertiary reference center) and the severity of arterial hypertension (stage I versus stage III) (Zennaro, Boulkroun and Fernandes-Rosa, 2020; Reincke *et al.*, 2021). Of note, PA is a world-wide problem and not limited to primarily Caucasian populations as revealed by a recent investigation from the CONPASS study group in China. In this study, 3.9 % of patients with newly diagnosed arterial hypertension had underlying PA (Xu *et al.*, 2020).

PA arises due to excessive autonomous and renin-independent adrenal aldosterone production (Reincke *et al.*, 2021). The first step to a diagnosis of PA is to screen for an increased aldosterone-to-renin-ratio. Screen positive patients are then submitted to one of the confirmatory testing protocols like the saline infusion test, the captopril challenge test and the fludrocortisone suppression test.

Since aldosterone excess may either originate from one or both adrenal glands, efforts to determine the PA subtype (i.e., unilateral or bilateral disease) once biochemical confirmation has been obtained, are crucial. As recommended by the Endocrine Society guidelines, lateralization is usually assessed by adrenal vein sampling (Funder *et al.*, 2016). Lateralization studies should be complemented by tomographic imaging. Patients with unilateral PA may undergo adrenalectomy of the affected gland with a high rate of cure or improvement of arterial hypertension. Bilateral disease is treated with lifelong administration of mineralocorticoid antagonists (Reincke *et al.*, 2021).

After surgical therapy, 98 % patients with unilateral forms of PA achieve a normalization of aldosterone excess. However, arterial hypertension is completely alleviated only in 37 % of these patients. Factors associated with partial or absent success (i.e., patients still having to take antihypertensive medication) are – amongst others – age of the patient and duration of arterial hypertension (Williams *et al.*, 2017). This suggests that while PA was still undiagnosed in these patients, their arterial system probably underwent substantial remodeling to an extent that is only incompletely reversible even after complete removal of aldosterone excess as the initial inciting stimulus.

Patients with bilateral forms of PA who are treated with mineralocorticoid antagonists have a worse prognosis than surgically treated patients with regards to cardiovascular end-organ damages (G. Hundemer *et al.*, 2018; G. L. Hundemer *et al.*, 2018b, 2018a). Reasons for this observation may reside in suboptimal patient adherence due to medication side effects such as gynecomastia and erectile dysfunction or physician inertia but may also reflect underlying steroid biology:

GPR30 transmembrane receptor-mediated effects of aldosterone have been demonstrated in smooth muscle cells (Gros *et al.*, 2011) and T-cells (Dinh *et al.*, 2020). It may, thus, be that MR antagonists do not block the full biological panoply of aldosterone effects. In addition to this, cortisol co-secretion has been described in primary aldosteronism (Arlt *et al.*, 2017). This additional steroid is probably only incompletely antagonized by current pharmacotherapy, leaving glucocorticoid receptor-mediated effects unopposed.

Despite numerous calls to action with the intention to raise awareness for PA in clinicians, PA still goes undiagnosed in most cases (Lubitz *et al.*, 2015; Reincke, 2018; Reincke *et al.*, 2021; Funder and Carey, 2022). This implies that a long duration of hypertension and subsequent remodeling with impaired recovery from arterial hypertension even after surgery will remain the general rule for this patient population. Finding new ways for adjuvant medical therapy to combat these remodeling processes at the level of the site of damage (endothelial cells), therefore, seems to be a reasonable strategy to provide a way to achieve complete clinical success after surgery and to minimize long term cardiovascular sequelae after initiation of medical therapy for PA.

### 1.1.2 Organ damage in PA

It is important to always consider PA as differential diagnosis and, if appropriate, to initiate a screening test. This is because patients with PA are more prone to exhibit cardiovascular sequelae and organ damages than patients with essential hypertension. Diseases include stroke (Milliez *et al.*, 2005; Ohno *et al.*, 2018), cerebral white matter lesions (Yuan *et al.*, 2021), atrial fibrillation (Milliez *et al.*, 2005; Savard *et al.*, 2013; Ohno *et al.*, 2018), coronary artery disease (Savard *et al.*, 2013; Ohno *et al.*, 2018) and myocardial infarction (Savard *et al.*, 2013), kidney damage as manifested by proteinuria (Monticone *et al.*, 2017; Ohno *et al.*, 2018) and left ventricular hypertrophy (Monticone *et al.*, 2017) and fibrosis (Freel *et al.*, 2012). The excess cardiovascular risk in PA is independent of the degree of arterial hypertension and, thus, commonly attributed to the elevated circulating aldosterone concentrations (Ohno *et al.*, 2018). In this context it is noteworthy that patients with PA are more likely than essential hypertensive control subjects to die from cardiovascular causes (Reincke *et al.*, 2012).

	<b>Stroke</b>	<b>Atrial fibrillation</b>	<b>Coronary artery disease</b>	<b>Proteinuria</b>
<b>PA</b>	7 %	4 %	4 %	15 %
<b>EH</b>	3 %	1 %	1 %	6 %

**Table 1:** Cardiovascular damage in patients with primary aldosteronism (PA) compared to patients with essential hypertension (EH). Patients were matched for age, sex and blood pressure. Data according to Ohno *et al.*, 2018.

An additional finding which has been replicated in independent cohort studies is that patients with primary aldosteronism exhibit an increased pulse wave velocity as a marker of reduced vascular compliance (Štrauch *et al.*, 2006; Bernini *et al.*, 2008; Lin *et al.*, 2012; Hung *et al.*, 2019; Chan *et al.*, 2020). Also, reduced flow-mediated dilation as a marker for endothelial function has been described in a number of papers on mostly Japanese PA cohorts (Nishizaka *et al.*, 2004; Tsuchiya, Yoshimoto and Hirata, 2009; Hannemann *et al.*, 2011; Matsumoto *et al.*, 2015; Kishimoto *et al.*, 2018, 2020; Takeda *et al.*, 2018; Watanabe *et al.*, 2021).

Finally, a unifying theme of the above-mentioned cardiovascular sequelae of PA is that they are all associated directly or indirectly with atherosclerosis. The current understanding of the pathophysiology of atherosclerosis, on the other hand, is a sequence of events which starts with endothelial dysfunction which designates a functional impairment of the innermost luminal cellular layer of blood vessels (Gimbrone and García-Cardeña, 2016). In other words, one of the primary steps, if not the root cause of cardiovascular sequelae (not only in PA) is endothelial dysfunction. Endothelial dysfunction is considered to be the earliest measurable manifestation of atherosclerosis and predicts progression to measurable later stages such as an increased carotid intima-media thickness (Halcox *et al.*, 2009) and major adverse cardiovascular events (Chan *et al.*, 2003). But not only does endothelial dysfunction hold a role early in the disease course of atherosclerosis; it is also crucial for the subsequent progression to plaque disease, plaque erosion and its ultimate devastating complication, arterial thrombosis (Gimbrone and García-Cardeña, 2016). The goal of this thesis was, therefore, to come to potential therapeutic applications by a deeper investigation of a specific endothelial pathway, the release of epoxyeicosatrienoic acids (EETs) in the context of aldosterone excess.

## 1.2 Endothelial factors

### 1.2.1 Overview

Vascular tone is the result of a balance between factors which promote smooth muscle constriction and (mostly endothelium-derived) factors which mediate smooth muscle relaxation (Féletalou and Vanhoutte, 2009). Commonly used *ex vivo* models to investigate endothelial function are isobaric and isometric arteriography which involve intact preparations of living arteries and registration of diameter or tone as readout. After inducing vasoconstriction an endothelial stimulant like acetylcholine is applied and the resulting vasodilation (increase in diameter or loss of tone) is noted (Mulvany and Aalkjaer, 1990).

Among the endothelium-derived vasodilators nitric oxide (NO) is probably the factor which is most readily associated with endothelial function since the Nobel Prize in Physiology or Medicine was awarded to Furchtgott, Ignarro and Murad in 1998 for their individual contributions to elucidate the role of nitric oxide in the cardiovascular system (Furchtgott and Zawadzki, 1980). Another potent endothelium-derived vasodilator is cyclooxygenase-mediated generation of prostacyclin (PGI<sub>2</sub>) (Moncada and Vane, 1978). However, vasodilation in response to endothelial stimulation can still occur in conditions in which endothelial nitric oxide and prostacyclin synthesis are inhibited. A multitude of endothelium-derived factors and mechanisms which mediate vasodilation under these circumstances have been identified and are summarized under the umbrella term endothelium-derived hyperpolarizing factor (EDHF). Among these are the release of potassium via SK<sub>Ca</sub> and IK<sub>Ca</sub> channels (Edwards *et al.*, 1998), hydrogen peroxide (Matoba *et al.*, 2000), and arachidonic acid-derived epoxyeicosatrienoic acids (EETs) (Campbell *et al.*, 1996). **Figure 1** provides an overview on a selection of endothelium-derived factors and mechanisms.

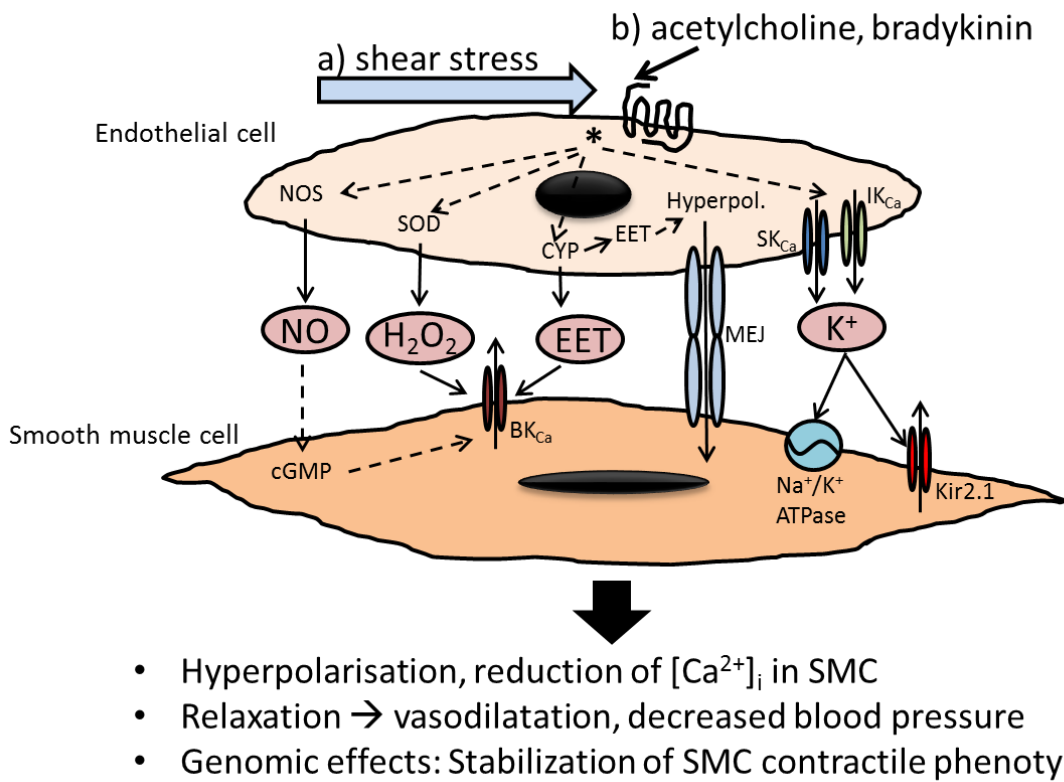


**Figure 1.** Overview of selected factors secreted by endothelial cells in response to either mechanical (shear stress) or chemical (acetylcholine, bradykinin) stimuli and their action on underlying smooth muscle cells. All stimuli converge on an elevation in endothelial cytosolic calcium (\*). This then mediates activation of nitric oxide synthase (NOS) which generates NO which in turn elevates smooth muscle cGMP. Calcium is also critical to activate superoxide dismutase (SOD) for the generation of H<sub>2</sub>O<sub>2</sub>, and for the activation of CYP epoxygenases for the synthesis of EETs. A lot of endothelial factors mediate smooth muscle relaxation by activating BK<sub>Ca</sub> channels (NO, H<sub>2</sub>O<sub>2</sub>, EETs), others act by direct passage of hyperpolarizing currents (myoendothelial junctions, MEJ) and by activating sodium-potassium ATPase and inward rectifying potassium channels (Kir2.1) (release of K<sup>+</sup>). The mechanism of EETs is still not fully resolved and may either involve a direct action on smooth muscle or an auto-stimulation of endothelial cells with subsequent release of hyperpolarizing factors or passage of hyperpolarizing currents to smooth muscle via MEJ. Endothelium-derived vasodilators not only acutely dilate vessels but also stabilize the normal smooth muscle contractile phenotype, thereby preventing a pro-atherogenic synthetic phenotype switch.

### 1.2.2 Epoxyeicosatrienoic acids (EETs)

The seminal works of William Campbell and colleagues uncovered that arachidonic acid relaxed bovine coronary arteries by CYP450-dependent conversion to EETs (Rosolowsky and Campbell, 1993). He then showed that EETs were by the endothelium to hyperpolarize underlying smooth muscle, thereby fulfilling the criteria for an EDHF (Campbell *et al.*, 1996). Their findings were complemented by experiments demonstrating the transferable nature of EETs by using a reporter assay (endothelium-intact arteries as EET donors and endothelium-denuded arteries as detectors) (Gauthier *et al.*, 2005). Ingrid Fleming and co-workers advanced the field by showing that CYP450 2C isoenzymes were critical in mediating EDHF in porcine coronary arteries (Fisslthaler *et al.*, 1999) whereas Darryl Zeldin and his group demonstrated that the

synthesis of EETs in the human heart is mediated by CYP2J2 (Wu *et al.*, 1996). Further studies could confirm that human coronary arteries also release EETs and that EETs also act as vaso-dilators in human vessels (Archer *et al.*, 2003; Larsen *et al.*, 2006). It should also be noted that endothelial EETs might activate endothelial TRPV4 channels in an autocrine manner (Watanabe *et al.*, 2003; Vriens *et al.*, 2005) which should then induce the release other “classical” mediators such as nitric oxide which subsequently relax smooth muscle cells.

Similar to the vascular balance of contractile and relaxing factors, the biological activity of EETs is controlled by their rate of synthesis and release versus their rate of metabolism by epoxide hydrolases. These enzymes catalyze hydrolysis of the epoxide bond and convert EETs to dihydroxyeicosatrienoic acids (DHETs). Soluble epoxide hydrolase (sEH, the human gene symbol being EPHX2) is arguably the most important isoenzyme to mediate EET hydrolysis *in vivo* (Imig, Jankiewicz and Khan, 2020), although studies in knock-out mice revealed that microsomal epoxide hydrolase (mEH, the human gene symbol being EPHX1) may have a distinct role in regulating EET bioavailability:

Baseline EET production is counterbalanced by mEH which sits in close proximity to CYP2C8 and CYP2C9 epoxygenases. When EET production is increased, as it has been shown in cardiac post ischemic reperfusion, EET hydrolysis is mediated by sEH because mEH is saturated. The specific role for mEH, therefore, seems to be in baseline EET production whereas sEH serves to regulate EET bioavailability in situation requiring an acute increase in EET synthesis (Edin *et al.*, 2018).

CYP 2C8 and CYP2J2 staining, on the other hand, was more prominent in endothelial cells, whereas CYP2C9 signals were homogenously distributed across the whole vessel wall (Larsen *et al.*, 2006). CYP2C8 and CYP2J2 expression, therefore, seems to be rather endothelial cell-specific.

Immunofluorescence studies have mapped the expression of sEH mostly to medial smooth muscle cells of intrarenal arteries, supporting the view that EETs are eliminated by the cells designated to be influenced by their release (Yu *et al.*, 2004). Other researchers found that sEH expression localizes mostly to endothelial cells in human coronary arteries (Larsen *et al.*, 2006). The cellular origin of vascular and, specifically, coronary vascular sEH activity is, thus, not completely resolved.

In a study involving mouse brains, Marowsky and colleagues described mEH expression in both endothelial and smooth muscle cells of intraparenchymal arterioles (Marowsky *et al.*, 2009).

**Figure 2** summarizes the four EET regioisomers, their four degradation products (DHETs) and the cellular origin of their main metabolizing enzymes.

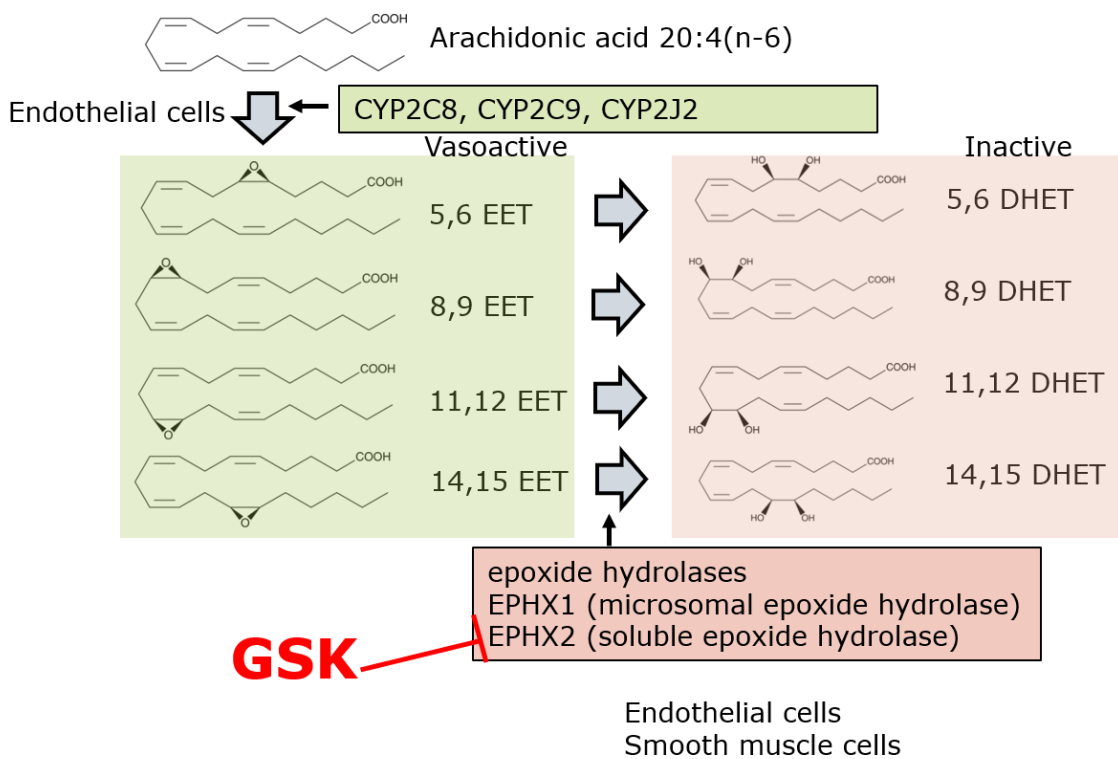


**Figure 2.** Generation and degradation of EETs in vascular cells. Upon release of arachidonic acid, EETs (green box) are generated by CYP epoxygenases in endothelial cells. They are inactivated to DHETs (red box) by microsomal epoxide hydrolase (mEH, EPHX1) and soluble epoxide hydrolase (sEH, EPHX2) expressed in both endothelial and smooth muscle cells. EPHX2 can be inhibited pharmacologically by GSK 2256294 (GSK).

Treatment of endothelial cells with compounds which directly increase cytosolic calcium (such as the ionophore A23187 (Fang, Weintraub and Spector, 2003)) or which indirectly increase calcium by mechanisms after binding to a G-protein coupled receptor (such as acetylcholine (Archer *et al.*, 2003) or bradykinin (Gauthier *et al.*, 2005)) induced a measurable increase in extracellular EETs. Likewise, cyclic stretch has been shown to induce EET release from coronary arteries as well as cultured endothelial cells (Fisslthaler *et al.*, 2001).

Two alternative hypotheses are proposed to explain increases in extracellular EETs after endothelial cell stimulation (Imig, 2012): Increases in calcium stimulate phospholipase A<sub>2</sub>, which releases arachidonic acid from membrane-bound phospholipids. CYP epoxygenases then convert arachidonic acid into EETs which then are released and hyperpolarize underlying smooth muscle by activating BK<sub>Ca</sub> channels. Alternatively, EETs are preformed and stored as membrane phospholipids until their release by a calcium-activated phospholipase (Spector *et al.*, 2004). The latter hypothesis should allow for a quicker onset of EET-mediated actions due to their instantaneous availability upon stimulation.

### 1.2.3 Intersection of EETs and primary aldosteronism

Several lines of evidence prompted us to investigate the role of EETs in primary aldosteronism:

The biological importance of nitric oxide as endothelial vasodilator diminishes with ageing: A study using young (<30 years) and elder (>60 years) human athletes and sedentary subjects discovered that all vasodilation in elderly, sedentary subjects is due to non-nitric oxide-mediated

pathways (Taddei *et al.*, 2000). The median age of patients with PA in a recent overview of the German Conn's registry was 51 years and while their body mass index (BMI) was 27.8 kg/m<sup>2</sup> (Heinrich *et al.*, 2018), suggesting a rather sedentary pattern in patients with PA. Integrating these two observations suggests that non-nitric oxide-mediated vasodilation might be the predominant pathway in patients with PA. However, most research on endothelial dysfunction in PA focused on NO (Nagata *et al.*, 2006; Leopold *et al.*, 2007; Oberleithner *et al.*, 2009; Favre *et al.*, 2011). The role of EDHF and, specifically, of EETs has barely been touched on so far.

An early hint in this direction showed that the development of arterial hypertension in rats treated with the mineralocorticoid precursor deoxycorticosterone acetate (DOCA) and sodium chloride could be halted once an inhibitor of sEH was administered (Loch *et al.*, 2007). Two studies on human cohorts described that serum levels of 14,15-DHET (the inactive sEH product of 14,15-EET hydrolysis) were positively correlated with the degree of abdominal aortic calcification and serum aldosterone levels, suggesting that EETs might play a protective role in aldosterone-mediated vascular calcification (Liu *et al.*, 2018).

Luther *et al.* demonstrated that subtype specific treatment of PA results in an increase in plasma EETs while in their study no change in DHETs was observed (Luther *et al.*, 2021). Because these results imply that PA rather impairs EET synthesis than their hydrolysis they stand in opposition to the findings of Liu *et al.* Furthermore, the above-mentioned findings cannot provide evidence on the cellular origin of EETs i.e., whether endothelial or, as also described, red blood cells (Jiang, Anderson and McGiff, 2010) are the source of circulating EETs.

A structured investigation of the impact of aldosterone excess on EET secretion in an endothelial cell culture system, thus, seemed warranted.

### 1.3 Corticosteroid receptor transactivation

The mineralocorticoid receptor, despite its name, does not show ligand selectivity: Glucocorticoids can activate the MR and lead to the same downstream effects as aldosterone, a feature which becomes evident in patients with glucocorticoid excess who develop arterial hypertension with an initial prevalence of 58-85 % (Braun, Vogel and Reincke, 2022). But also under normal physiological conditions the so-called MR transactivation by glucocorticoids is relevant and due to the following biochemical facts:

First, plasma concentrations of cortisol are 100- to 1000-fold higher than those of aldosterone (Chapman, Holmes and Seckl, 2013). Second, cortisol also has a 20 fold higher affinity to the human MR than for human GR (Hellal-Levy *et al.*, 1999).

Early studies established that kidney and colon had the highest conversion of cortisol to cortisone. In these tissues, pharmacological inhibition of 11- $\beta$ -HSD type 2 with carbenoxolone yielded a substantial increase of radiolabelled glucocorticoid binding in vivo (Funder *et al.*, 1988). In agreement with these findings, Carl Monder and his group demonstrated that conversion of corticosterone to 11-dehydroxycorticosterone (the analogous glucocorticoid inactivation step in rodents) was greatest in rat kidney and mostly mediated by distal tubular fractions. When kidney sections were incubated with glycyrrhetic acid, another inhibitor of 11- $\beta$ -HSD type 2, the binding of radiolabeled corticosterone increased and resembled the bindings pattern of labeled aldosterone (Edwards *et al.*, 1988). Together, these studies provided first evidence of a tissue-specific pre-receptor mechanism to limit the degree of MR ligand promiscuity, i.e., to restrict MR activation to mineralocorticoids and exclude glucocorticoids from such activity (**Figure 3**).

These basic studies were complemented by investigations on human congenital 11- $\beta$ -HSD type 2 deficiency (apparent mineralocorticoid excess) (Stewart *et al.*, 1988) and normal subjects who ingested licorice, known to harbor mineralocorticoid activity which was presumed to be exerted by glycyrrhetic acid (Stewart *et al.*, 1987). In both studies a significant increase in the urinary (tetrahydrocortisol+allo-tetrahydrocortisol)/tetrahydrocortisone ratio, a finding compatible with decreased conversion of cortisol to cortisone, was apparent.

The current thinking is that in tissues with low expression levels of 11- $\beta$ -HSD type 2 under baseline conditions most MR should be occupied by cortisol. Any additional amounts of cortisol, i.e. during stress, should bind directly to GR. By these mechanisms it is ensured that the glucocorticoid signal transduction during stress is confined to the GR (Hartmann *et al.*, 2021) but it also underlines that tissues may exhibit striking differences in baseline mineralocorticoid signaling. In line with these thoughts, many of the interactions between gluco- and mineralocorticoid signaling seems to be highly tissue-specific. In the following paragraph examples of tissues with little to no protection of MR from circulating glucocorticoids will be given.

Hartmann and colleagues provided a model how the stress response in hippocampal neurons is orchestrated by the interaction of MR expression levels which modulate the GR-dependent response to surges in glucocorticoids (Hartmann *et al.*, 2021). In their experiments, the baseline expression levels of mineralocorticoid receptors determined the subsequent response stress response. They finally concluded that mineralocorticoid receptor activation in the hippocampus leads to an increased synthesis of the inhibitory GR chaperone FKBP5 which in turn impairs the nuclear translocation of glucocorticoid-GR complexes during the stress response.

Mihailidou and co-workers described that in experimental myocardial infarction both cortisol and aldosterone increased infarct size and apoptosis in a manner sensitive to spironolactone. Because the beneficial effects of spironolactone were mimicked by administration of the superoxide dismutase mimetic tempol (an antioxidant), the investigators concluded that both aldosterone and cortisol effects were mediated by oxidative stress (Mihailidou *et al.*, 2009).

Hadoke and colleagues examined contractile responses of thoracic aortas from both 11- $\beta$ -HSD type 1 and type 2 gene-deficient (KO) mice in comparison to wild type controls. Only the 11- $\beta$ -HSD type 2 KO aortas depicted endothelial dysfunction which manifested as exaggerated contractile response to norepinephrine and reduced acetylcholine-mediated vasodilation which both disappeared by endothelial denudation (Hadoke *et al.*, 2001). In a further study, the same group demonstrated that treatment of the same mice with corticosterone induced no change in endothelial or smooth muscle function in both wild type and mutated animals (Christy *et al.*, 2003). Together, these results suggest that for mouse endothelial cells, 11- $\beta$ -HSD type 2 may not play a huge role as a prereceptor modulator of MR accessibility to glucocorticoids *in vivo*. The mechanism of endothelial dysfunction in 11- $\beta$ -HSD type 2 KO mice remains to be resolved.

11- $\beta$ -HSD type 1 has been shown to catalyze either the conversion of cortisone to cortisol (hydrogenase/oxo-reductase) or the reverse reaction (dehydrogenase). Availability of the co-substrate NADPH (mostly generated by closely located hexose-6-phosphate dehydrogenase) is required for the oxoreductase activity. Hence, NADPH concentrations probably influence the substrate flow by 11- $\beta$ -HSD type 1 (Chapman, Holmes and Seckl, 2013).

On the other hand, 11- $\beta$ -HSD type 2 uses NAD<sup>+</sup> to function as a dehydrogenase, so reductions in this co-factor should negatively impact on the dehydrogenase activity of 11- $\beta$ -HSD type 2. Oxidative stress depletes NAD<sup>+</sup> in endothelial cells (Thies and Autor, 1991). This may serve as an explanation for the link between reactive oxygen species generated by mineralocorticoids

and the resulting cardiovascular damage via increased transactivation of MR by glucocorticoids as described in the above-mentioned study of Mihailidou (Mihailidou *et al.*, 2009).

While in colonic epithelial cells aldosterone was suggested to increase 11- $\beta$ -HSD type 2 expression (Fukushima *et al.*, 2005), this relationship remains speculative for endothelial cells since no data on this cell type are available.

In sum, while the enzymes 11- $\beta$ -HSD type 1 and type 2 have been shown to be expressed in endothelial cells, their contribution to steroid metabolism in this cell type under normal conditions as well as under conditions of aldosterone excess is currently not well understood.

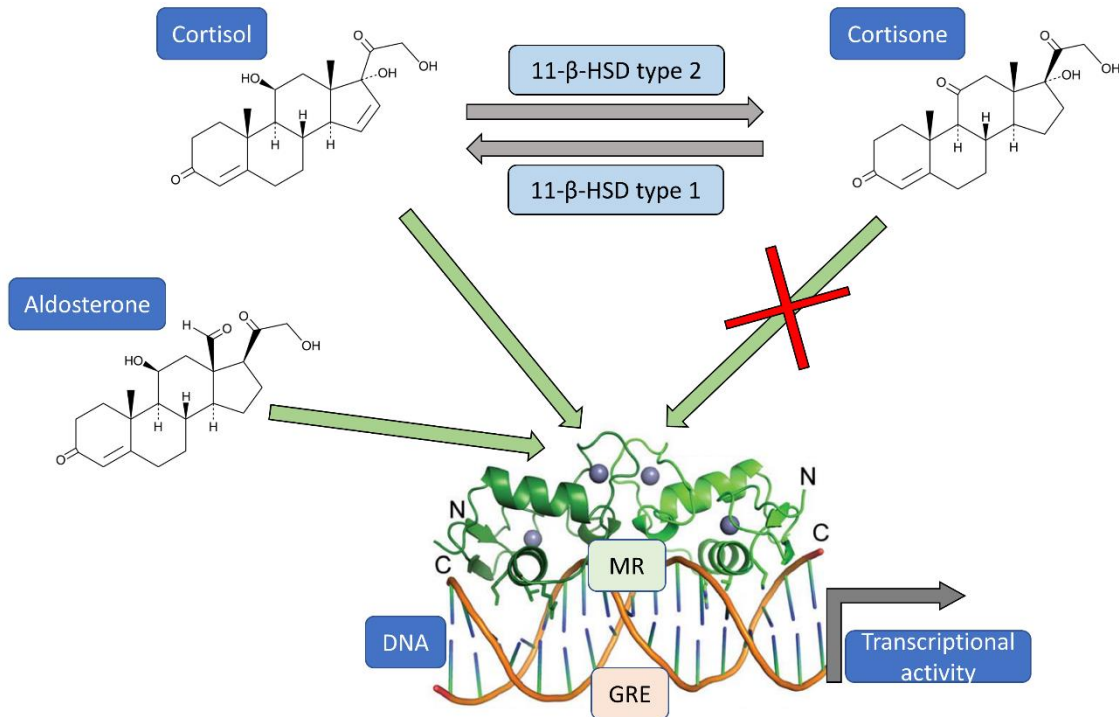


**Figure 3.** Tissue selective MR activation is controlled by cell type-specific expression levels of 11- $\beta$ -HSD type 1 and type 2. 11- $\beta$ -HSD type 2 catalyzes cortisol inactivation to cortisone while 11- $\beta$ -HSD type 1 catalyzes the reverse reaction. Cortisol and aldosterone bind to mineralocorticoid receptors (MR) while cortisone does not. MR-steroid complexes then translocate to the nucleus where they bind to glucocorticoid response elements (GRE) of accessible DNA. Figure modified according to Hudson, Youn and Ortlund, 2014.

Theoretically, the reverse transactivation process is also conceivable: Mineralocorticoids may activate glucocorticoid receptor in situations of aldosterone excess which could overcome naturally competing glucocorticoid concentrations. Rupprecht and co-workers calculated comparative induction activities of both cortisol and aldosterone for GR. Aldosterone at the level of GR induced a 200 fold maximum transcriptional activity, compared to a 700 fold induction by cortisol, indicating that theoretically transactivation of GR by aldosterone may occur (Rupprecht *et al.*, 1993). In the cited study, aldosterone at the GR displayed ED<sub>50</sub> values of 50 nM, a maximum stimulation would therefore be expected to occur at levels of ca. 250 nM, which even in primary aldosteronism are seen very rarely (Heinrich *et al.*, 2018).

Using a luciferase-GR reporter construct, Hellal-Levy *et al.* also demonstrated that aldosterone at concentrations found in vivo yields negligible transcriptional responses of the GR (Hellal-Levy *et al.*, 1999).

While the above-mentioned results from heterologous overexpression systems suggest that aldosterone should not display relevant GR binding, it is unclear to which degree these findings are applicable to cell systems which natively express GR and MR at physiological levels and are stimulated with (patho-)physiologically realistic steroid concentrations. Moreover, the induction of 11- $\beta$ -HSD type 2-mediated MR protection in mineralocorticoid excess, as proposed by Fukushima *et al.* (Fukushima *et al.*, 2005) remains to be demonstrated in endothelial cells.

We, therefore, decided to address these questions in human coronary artery endothelial cells as a pathophysiologically relevant end-organ for steroid effects.

## 1.4 Study aims

Part A of this study focused on the question to which degree culture conditions similar to primary aldosteronism would affect the endothelial EET system in terms of expression of critical enzymes which determine the concentrations of bioactive EETs. Another important component of part A was the direct measurement of stimulated release of free EETs into the culture medium under PA-like conditions. Ultimately, part A tried to answer the question whether endothelial dysfunction in PA may at least partly due to a defect in the endothelial EET pathway.

Part B of this study aimed to investigate the transactivation of gluco- and mineralocorticoid receptors in endothelial cells by mineralo- and glucocorticoid steroids. Another question to be answered was whether endothelial cells are capable of significant metabolism of cortisol and aldosterone and to which extent this would be modifiable by aldosterone excess.

## 2. Material and Methods

### 2.1 Cell culture and stimulation

#### 2.1.1 List of materials for cell culture

Material	manufacturer	Reference number
<b>Incubator</b>	Thermo Scientific	BBD 6220
<b>Hemacryptometer</b>	Bio-Rad	Tc20 Automated Cell counter
<b>Culture flask</b>	Cellstar	658175
<b>Basal medium endothelial cells</b>	Lonza	CC-3156
<b>Growth Medium-2 Single Quots™ Supplements and Growth Factors Kit for endothelial cells</b>	Lonza	CC-3202
<b>ReagentPack</b>	Lonza	CC-5034
<b>Trypsin/EDTA</b>	Lonza	CC-5012
<b>HEPES</b>	Lonza	50-5022
<b>TNS (Trypsin neutralizing solution)</b>	Lonza	CC-5002
<b>DPBS</b>	Gibco by life technologies	
<b>96-well plates</b>	Corning® Sigma Aldrich	
<b>6-well plates</b>	Cellstar, Greiner bio-one	657 160
<b>DMSO</b>	Sigma Aldrich	D8418-100ML
<b>Hydrocortisone</b>	Sigma Aldrich	H0888-1b
<b>Aldosterone 25 mg (dissolved in DMSO at 2 mM)</b>	Sigma Aldrich	A9477-25MG
<b>Eplerenone 10mg (solved in DMSO at 2 mM)</b>	Tocris	2397
<b>14,15-EET (dissolved in DMSO at 1 mM)</b>	Cayman chemicals	50651
<b>GSK 2256294A</b>	Axon Medchem	2307

Human coronary artery endothelial were purchased from Lonza (Basel, CH) together with their specific growth media and growth factors and were cultured in specific growth-medium with supplements according to the manufacturer's recommendations (details see below in section Drugs, buffer compositions, chemicals). All experiments were conducted between passages 5-9 and both cell lines were maintained at 37°C, 5% CO<sub>2</sub> and 95% O<sub>2</sub> in a humidified incubator. Cells were serum starved over night before treatment in EBM-2 medium as the confluence reached 85-90%. Pharmacological treatment was performed in serum-free medium for an additional 48 hours.

## 2.2 RNA extraction, reverse transcription and qPCR

### 2.2.1 List of materials for RNA extraction, reverse transcription and qPCR

Material	manufacturer	Reference number
<b>DPBS</b>	Gibco by life technologies	14190-094
<b>Cell-Scraper</b>	Sarstedt Cellscraper 25 cm	83.1830
<b>Centrifuge</b>	Eppendorf Centrifuge	5424
<b>Nano Drop</b>	PeqLab Nanodrop 1000	
<b>Maxwell-Kit</b>	Maxwell 16 LEV simply RNA cells kit	AS1280
<b>Proteinase K</b>	Thermofisher	EO 0492 (Stock, 0.25mg/ml)
<b>GoScript Reaction Buffer, Oligo(dT)</b>	Promega	A2791
<b>Go Script Enzyme Mix</b>	Promega	A5003
<b>Thermo Cycler</b>	PeqLab	
<b>ITaq universal super probes mix</b>	Bio-Rad	172-5134
<b>96 well plate</b>	Applied biosystems	4346907
<b>96 well plate cover</b>	Applied biosystems	4360954
<b>Nuclease-free water</b>	Promega	
<b>Centrifuge</b>	Eppendorf Centrifuge	5804
<b>Quant Studio 5 Real time PCR system</b>	Applied biosystems, Thermo Fisher	

### 2.2.2 RNA extraction

Total RNA was extracted using the Maxwell 16 LEV simply RNA cells kit (Promega, Walldorf, Germany). The manufacturer's protocol was tightly adhered to. Cells were harvested from 6-

well plates (using a scraper) in 1ml DPBS after treatment and were centrifuged at 1300 rpm and 21°C for 3 minutes. The resulting pellet was resuspended in 200 µl of chilled 1-Thioglycerol/homogenization solution with vortex until the pellet was completely dissolved. Then, another 200 µl of lysis buffer and 25 µl of proteinase K were added to the homogenate, followed by vigorous vortex for 15 seconds. The solution was then left at room temperature for 10 minutes. Following extraction of RNA with the Maxwell cartridge kit the RNA which includes removal of genomic DNA, the RNA was eluted with a final volume of 50 µl of nuclease-free water. Finally, the RNA yield was determined using a Nanodrop 1000 spectrophotometer (Thermo Fisher Scientific).

### 2.2.3 Reverse transcription

RNA was reversed transcribed using the GoScript™ Reverse Transcriptase Kit (Promega). 100 ng RNA were used as input.

To ensure dissociation of GC-rich templates, RNA was heated to 70 °C for 5 minutes and then rapidly cooled on ice prior to addition to the master mix.

The reaction for each reverse transcription contained:

Nuclease-Free Water	4 µl
GoScript Reaction Buffer, Oligo(dt)	4 µl
GoScript Enzyme Mix	2 µl
100 ng of RNA	x µl (as dictated by RNA concentration)
Nuclease-free-water	to a final volume of 20 µl

The reaction mix was placed in a thermocycler (Peqlab Primus 25) and the following sequence of temperature steps was run (each step once):

	Temperature	Duration
<b>Annealing</b>	25 °C	5 min
<b>Extension</b>	42 °C	60 min
<b>Heat inactivation of reverse transcriptase</b>	70 °C	15 min
<b>Storage</b>	4 °C	∞

The reaction mix was the diluted 1:10, aliquoted and stored at -20 °C until the qPCR was run.

### 2.2.4 Quantitative real-time PCR (qPCR)

Each individual qPCR reaction contained the following:

0.5 ng cDNA	1 µl
iTaq universal probes supermix	10 µl
Taqman probe (see Table 1 below)	1 µl

Nuclease-free water 8  $\mu$ l

The 96 well plate was then loaded into a QuantStudio 5 machine (Thermo Fisher Scientific). Each cDNA sample was assessed in triplicate. At least three independent repeats of each qPCR experiment were conducted. We used the  $2^{-\Delta CT}$  method to normalize the expression levels of each gene of interest to the geometric mean of two housekeeping genes (EIF2B1 and HPRT1). Each individual  $2^{-\Delta CT}$  value was then normalized to the mean values of the experimental control group (usually DMSO treatment).

Gene of interest	Taqman probe ID
ACTA2	Hs05005341_m1
CYP2C8	Hs00946140_g1
CYP2C9	Hs04260376_m1
CYP2J2	Hs00559374_m1
EPHX1	Hs01116806_m1
EPHX2	Hs00932316_m1
EIF2B1	Hs00426752_m1
FKBP5	Hs01561006_m1
HPRT1	Hs99999909_m1
HSD11B1	Hs01547870_m1
HSD11B2	Hs00388669_m1
NFKBIA	Hs00153283_m1
SCNN1A	Hs00168906_m1

**Table 2.** Genes of interest and corresponding Taqman probes used in the qPCR experiments

qPCR cycle properties were the following:

	Temperature	Duration	Cycles
<b>Polymerase activation</b>	95 °C	30 s	1x
<b>Denaturation</b>	95 °C	15 s	55x
<b>Annealing and extension</b>	60 °C	20 s	
<b>Storage</b>	4 °C	$\infty$	

## 2.3 Fluo4-based calcium imaging

### 2.3.1 Materials for calcium imaging

Material	manufacturer	Reference number
<b>Incubator</b>	Heraeus cell	
<b>HEPES buffer</b>		
<b>140 mM NaCl</b>	Sigma Aldrich	S9888
<b>5.4 mM KCl</b>	Merck	A746433 617
<b>1 mM MgCl</b>	Sigma Aldrich	M8266
<b>10 mM HEPES</b>	Sigma Aldrich	H4034
<b>10 mM Glucose</b>	Merck	
<b>2 mM CaCl<sub>2</sub> x 2H<sub>2</sub>O</b>	Sigma Aldrich	C-5080
<b>Fill up with distilled water to desired volume</b>		
<b>Adjust pH to 7.4 with NaOH</b>		
<b>Pass through 0.2 µm sterile filter</b>		
<b>BSA (bovine serum albumin)</b>	Sigma Aldrich	A3803-100G
<b>Fluo-4</b>	ThermoFisher	F23981
<b>Acetylcholine</b>	Sigma-Aldrich	A2661-25G
<b>A23187</b>	ThermoFisher	C7522
<b>Victor X4 plate reader</b>	Perkin Elmer	

### 2.3.2 Calcium imaging

This method has already been described in detail in our manuscript (Brunnenkant *et al.*, 2021): After 48 h treatment in a 96-well plate, endothelial cells were washed twice with 200 µl HEPES buffer (37 °C), and loaded for 2 hours at 37 °C with 5 µM of Fluo-4 diluted in HEPES buffer containing 0.1 % pluronic (v/v). After the incubation period, cells were washed with HEPES (50 µl). A Victor X4 plate reader was used to register Fluo4 fluorescence signals. The plate reader had two injectors for continuous registration of fluorescence before and after injection of treatments.

To account for potential autofluorescence of cells and treatments, cells without prior Fluo4-loading but with the same 48 h treatments were stimulated with the same concentrations of acetylcholine. Fluorescence of cells not loaded with Fluo4 was taken as background signal and was subtracted from the raw fluorescence readings of each Fluo4-loaded cell at corresponding time points, resulting in background-corrected fluorescence (F). Finally, F at each time point was normalized to F at timepoint 0 (F<sub>0</sub>) resulting in F/F<sub>0</sub>.

Steady state  $F/F_0$  values in response to each acetylcholine concentration were taken as the final readout to calculate concentration response curves.

## 2.4 Stimulation of endothelial EET release

As described in detail in the supplement of our pre-print publication (Brunnenkant *et al.*, 2021), endothelial cells were synchronized under serum-free conditions over night, followed by treatment in serum-free medium for another 48 hours. Then, cells were washed with HEPES buffer and incubated with 10  $\mu$ M arachidonic acid in HEPES followed by stimulation with acetylcholine (1 or 100  $\mu$ M) dissolved in HEPES buffer. Cell-free supernatants containing secreted EETs and DHETs were then collected and kept at -80 °C until downstream HPLC-MS/MS was performed.

## 2.5 Quantification of EETs and DHETs in endothelial supernatant

HPLC MS/MS measurements were performed by a collaboration partner, Jair Gonzalez Marques, MSc., in the laboratory of Professor Dr. Berthold Koletzko in Munich. Jair Gonzalez Marques kindly provided his consent for the results to be used in this thesis.

The description pertaining to the HPLC MS/MS method follows closely that in our published manuscript (Brunnenkant *et al.*, 2021):

2.5 mL of supernatant were spiked with 20  $\mu$ L of 12.5 ng/mL 11,12-DHET-d11 and 25.0 ng/mL 11,12-EET-d11 (both from Cayman Chemical, Michigan, USA). Subsequently, 1000  $\mu$ L of dichloromethane (DCM) were added to extract lipids followed by 10 seconds of vigorous mixing. After separation of phases, the lower phase was again subjected to DCM extraction in another reaction vial in order to increase the yield. Extracts were then dried at 40°C before reconstitution in 100  $\mu$ L of methanol. Reconstituted samples were then transferred to a 96 well plate and dried under a nitrogen stream. Finally, 50  $\mu$ L of the initial HPLC mobile phase (see below) were added to reconstitute samples.

### 2.5.1 High performance liquid chromatography with tandem mass spectrometry (HPLC-MS/MS)

Chromatography was performed with a 1290 Infinity II high performance liquid chromatography (HPLC) system (Agilent Technologies, Waldbronn, Germany) in gradient mode. Analyst software (Version 1.7.0, AB Sciex, Darmstadt, Germany) was used as software interface. For chromatography a XBridge® C18 column (2.1 x 150 mm, 3.5  $\mu$ m) (Waters, Ireland) was used at 40°C.

The following mobile phase compositions and instrument settings were used:

Mobile phase (A): HPLC-grade water with 0.1% formic acid

Mobile phase (B): 1:1 mixture of methanol and acetonitrile with 0.1% formic acid

Flow rate: 1.3 mL/min

Injection volume: 10  $\mu$ L

The mobile phase gradient program was as follows:

Time (minutes)	Mobile phase (A)	Mobile phase (B)
0.0 – 0.1	60 %	40 %
0.2 – 3.8	30 %	70 %
3.9 – 4.4	1 %	99 %
4.5 – 5.5	60 %	40 %

Mass spectrometry experiments were carried out on a QTRAP® 6500+ machine coupled to a Turbo VTM ion source (AB Sciex, Darmstadt, Germany). Analyst Software was used as software interface for instrument operation and data acquisition.

The reader is referred to **Table 3** for analyte-specific MS transitions and parameter settings.

	Q1 mass (Da)	Q3 mass (Da)	CE (V)	RT (min)	DP (V)	CXP (V)
<b>5,6-EET</b>	319.00	191.00	-16	3.66	-70	-27
<b>8,9-EET</b>	319.00	154.90	-16	3.39	-85	-15
<b>11,12-EET</b>	319.00	208.00	-16	3.18	-50	-19
<b>14,15-EET</b>	319.00	219.10	-14	2.83	-65	-15
<b>5,6-DHET</b>	337.00	145.00	-26	1.92	-95	-19
<b>8,9-DHET</b>	337.00	127.00	-28	1.64	-65	-21
<b>11,12-DHET</b>	337.00	167.10	-24	1.49	-45	-15
<b>14,15-DHET</b>	337.00	207.00	-24	1.13	-60	-11

**Table 3.** Q1 fragment mass (Q1 mass), Q3 fragment mass (Q3 mass), collision energy (CE), retention time (RT), declustering potential (DP), and cell exit potential (CXP) for the mass spectrometric detection of quantifier transitions of EETs and DHETs.

## 2.6 Determination of steroids in endothelial culture supernatants

HPLC MS/MS measurements were performed by a collaboration partner, Sonja Kunz, MSc., in the laboratory of Dr. Martin Bidlingmaier in Munich. Sonja Kunz kindly provided her consent for the results to be used in this thesis.

Steroids in cell culture supernatant were quantified using a 1290 Infinity II high pressure liquid chromatography (HPLC) system (Agilent Technologies, Waldbronn, Germany) coupled to a QTrap 6500+ triple quadrupole mass spectrometer (MS/MS) (AB Sciex, Darmstadt, Germany).

Extraction of the steroids was performed by liquid-liquid extraction (LLE) with 1.5 mL methyl-tert-butyl-ether (MTBE) added to 1 mL of cell culture supernatant. The extract was concentrated by N<sub>2</sub> stream-assisted evaporation and reconstituted in 200 µL 50% methanol. 20 µL of the concentrated extract were injected to the HPLC-MS/MS system. Calibration solutions in 50% methanol and quality control samples in EBM-2 cell culture medium were freshly prepared before each measurement. Deuterated analogues of the steroids were used as internal standards,

to correct for analyte losses during the preparation and measuring process. The reader is referred to **Table 4** for analyte-specific transitions and parameters.

	Q1 mass (Da)	Q3 mass (Da)	CE (V)	RT (min)	DP (V)	CXP (V)
<b>Cortisol d4</b>	367.2	121	30	1.8	40	14
<b>Cortisol</b>	363.2	121	30	1.9	40	14
<b>Cortisol qualifier 1</b>	363.1	109	34	1.8	40	14
<b>Cortisol qualifier 2</b>	363.1	97	29	1.8	40	14
<b>Cortisone d8</b>	369.2	168.1	32	2.2	40	14
<b>Cortisone</b>	361.1	163.1	31	2.2	40	14
<b>Cortisone qualifier 1</b>	361.1	121	36	2.2	40	14
<b>Cortisone qualifier 2</b>	361.1	105	39	2.2	40	14
<b>Aldosterone d7</b>	369.2	323.2	29	2.8	40	14
<b>Aldosterone</b>	361.2	343.2	23	2.9	40	14
<b>Aldosterone qualifier 1</b>	361.2	315.2	27	2.9	40	14
<b>Aldosterone qualifier 2</b>	361.2	325.2	27	2.9	40	14

**Table 4.** Q1 fragment mass (Q1 mass), Q3 fragment mass (Q3 mass), collision energy (CE), retention time (RT), declustering potential (DP), and cell exit potential (CXP) for the mass spectrometric detection of quantifier, qualifier and internal standard transitions of aldosterone, cortisol and cortisone.

## 2.7 Immunofluorescence of endothelial cells

### 2.7.1 Materials for immunofluorescence

Material	manufacturer	Reference number
<b>Paraformaldehyde</b>	ThermoFisher Scientific	AAJ19943K2
<b>Triton X-100</b>	Sigma Aldrich	T8787-250ML
<b>BSA</b>	Sigma Aldrich	A3803-100G
<b>PBS</b>		
<b>Vectashield Mounting Medium with DAPI</b>	Vectorlabs	H-1500
<b>GR/NR3C1 antibody (BuGR2)</b>	Biotechne/NovusBio	NB 3000-731
<b>MR/NR3C2 antibody</b>	Biotechne/NovusBio	NBP2-57853

<b>α-actin antibody clone 1A4</b>	Sigma Aldrich		A2547
<b>Alexa 488 donkey anti-mouse IgG H+L</b>	Invitrogen Scientific		A-21202
<b>Alexa 594 donkey anti-rabbit IgG H+L</b>	Invitrogen Scientific		A-21207
<b>8 well slides</b>	Sarstedt		94.6150.801
<b>Fluorescence microscope</b>	Leica Microsystems		Leica DM 2500

Endothelial cells were seeded in 8 well slides at a density of 8000 cells/well. After 48 h of treatment they were washed with PBS, fixed for 30 minutes with 4% paraformaldehyde, washed again with PBS and permeabilized for 30 minutes with 0.5 % Triton X-100. Subsequently, non-specific binding sites were saturated with 1% BSA in PBS for 30 minutes. After this, the cells were incubated with a mixture of both primary antibodies (anti-GR and anti-MR antibody both at a dilution of 1:100) over night. The following day, the cells were washed again with PBS and a mixture of both secondary antibodies was applied (Alexa Fluor 488 donkey anti-mouse IgG; Alexa Fluor 594 goat anti-mouse IgG; both at 1:200) at room temperature for 1 hour. After a final 3 washing steps with PBS, cells were then embedded in mounting medium containing DAPI. Images were then acquired using a Leica TCS SP5 fluorescence microscope (Leica Microsystems, Wetzlar, Germany). Images were acquired using the same settings for exposure and gain. Images encompassing at least three well visible cells per treatment were registered at 40x magnification. Images were analyzed using Fiji, an open source software package of ImageJ2 (Schindelin *et al.*, 2012): The nuclear region, i.e. the DAPI-positive areas, were selected using the freehand tool in Fiji and saved as regions of interest using the ROI manager. Then the corresponding images for GR and MR were opened and the aforementioned ROIs were applied to these images. Subsequently, the mean grey value for both GR and MR within the ROIs was calculated. Values were then normalized to the mean of DMSO treated cells and expressed as mean  $\pm$  SEM.

## 2.8 Statistics

GraphPad Prism 8 (GraphPad Software, San Diego, CA, USA) was used for construction of graphs and computation of statistical significances. Bar graphs show mean  $\pm$  SEM. Statistical tests comprised Mann Whitney U tests, t-tests, 1-Way ANOVA or 2-Way ANOVA followed by indicated post hoc tests, wherever applicable. Statistical significance levels were set to a two-sided p-value of  $<0.05$ .

### 3. Results

#### 3.1 Part A: Endothelial eicosanoids in aldosterone excess

The following results have been published online on a pre-print server (<https://doi.org/10.1101/2021.02.04.429624>). The findings are also part of a manuscript submitted for publication.

##### 3.1.1 EET-related mRNA expression data in endothelial cells

To demonstrate the pathological significance of the aldosterone concentrations used, we assessed the expression of the mesenchymal phenotype marker ACTA2, the gene coding for smooth muscle  $\alpha$ -actin. Treatment with aldosterone, with or without concomitant hydrocortisone, led to an increased expression of  $\alpha$ -actin (**Figure 4**) which may indicate underlying endothelial to mesenchymal transition. This phenotype switch in turn has been linked to the development of atherosclerosis, amongst other cardiovascular diseases (Kovacic *et al.*, 2019).

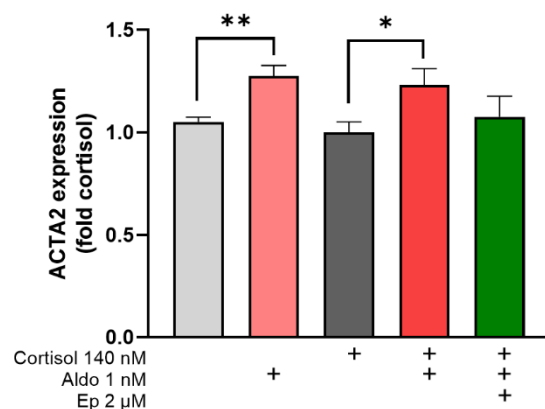


**Figure 4.**  $\alpha$ -actin (ACTA2) mRNA expression in human coronary artery endothelial cells as a marker of endothelial to mesenchymal transition in response to 48 hours of stimulation with the indicated treatments. Aldo, aldosterone, Ep, eplerenone; n=3-6 independent replicates per treatment; \*: p<0.05, \*\*p<0.01, t-test.

EETs are reported to be synthesized by Cytochrome P 450 epoxygenases. In humans, CYP2C8, CYP2C9 and CYP2J2 have been linked to this process (Zeldin *et al.*, 1995; Wu *et al.*, 1996; Imig, Jankiewicz and Khan, 2020). The concentration of synthesized EETs is counterbalanced by their degradation to DHETs which is mediated by epoxide hydrolases (Sinal *et al.*, 2000; Edin *et al.*, 2018). The relevant enzymes for this are mostly soluble epoxide hydrolase (the coding gene being EPHX2) and, to a lesser degree, microsomal epoxide hydrolase (the gene being EPHX1).

We could not detect mRNA for CYP2C9 in human coronary artery endothelial cells. Expression of CYP2C8 and CYP2J2 was low but detectable. Expression of CYP2C8, CYP2J2, EPHX1 and EPHX2 was not altered by treatment with aldosterone when compared to vehicle (DMSO)-

treated control cells. Co-stimulation of cells with aldosterone and hydrocortisone neither induced a differential expression of any of the aforementioned genes (**Figure 5**).

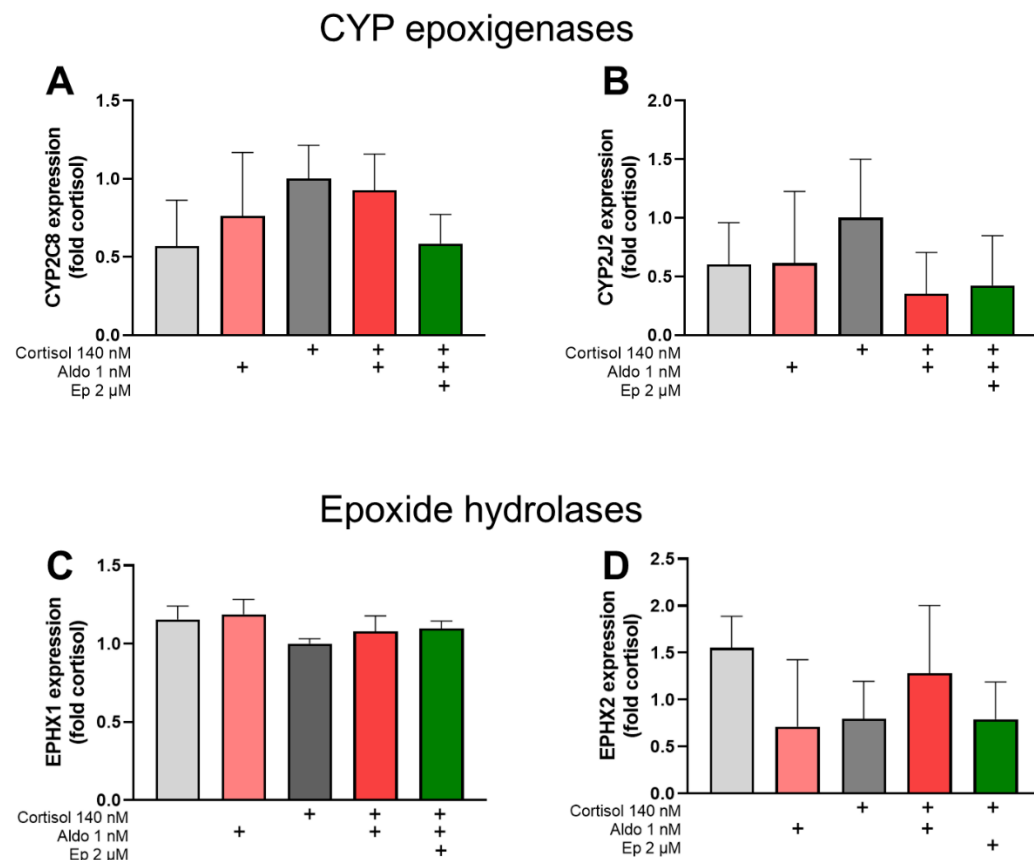


**Figure 5.** Gene expression patterns of CYP epoxigenases required for EET synthesis (**A**, CYP2C8; **B**, CYP2J2) and expression patterns of epoxide hydrolases required for inactivation of EETs (**C**, EPHX1 [mEH]; **D**, EPHX2 [sEH]) in human coronary artery endothelial cells in response to 48 hours of stimulation with the indicated treatments. Aldo, aldosterone, Ep, ep-lerenone; n=3 independent replicates per treatment.

We next addressed the consequences of aldosterone excess for endothelial function. To this end, we measured acetylcholine-induced increases in endothelial cytosolic calcium concentration using Fluo4 as calcium probe. Concentration response curves were constructed for acetylcholine under various treatment conditions. Since the release of endothelial vasodilators is preceded by an increase in cytosolic calcium (Falcone, 1995), we took the magnitude of the calcium response as marker for overall endothelial functional integrity. Earlier studies demonstrated that acetylcholine-induced increases in cytosolic calcium are concentration-dependent (Huang *et al.*, 2000; Zuccollo *et al.*, 2019). **Figure 6** shows example fluorescence traces in response to acetylcholine concentrations.

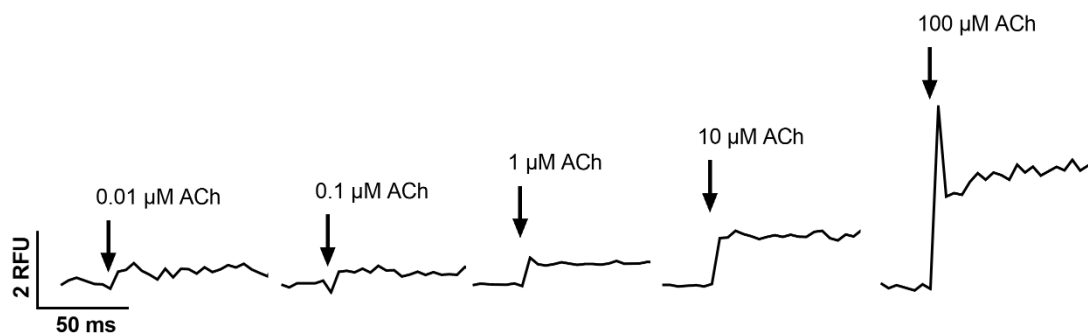


**Figure 6.** Example tracings of Fluo4 calcium signals in endothelial cells over time in response to the different acetylcholine concentrations used. ACh, acetylcholine; RFU, relative fluorescence units ( $F/F_0$ ).

Interestingly, the solvent-treated cells showed the lowest calcium response of all studied treatment conditions. The strongest response was observed in cells treated with physiological cortisol concentrations. Treatment with aldosterone and cortisol attenuated the response significantly. Addition of eplerenone to aldosterone and cortisol resulted in a curve which showed a trend towards normalization. This, however, did not reach statistical significance (Figure 7). In sum, the aldosterone concentration used resulted in a measurable deficit of endothelial cell calcium response as a marker of endothelial dysfunction. Since cortisol-treated cells showed the strongest response and untreated cells the weakest, we decided to subsequently use cortisol treatment as the control condition.

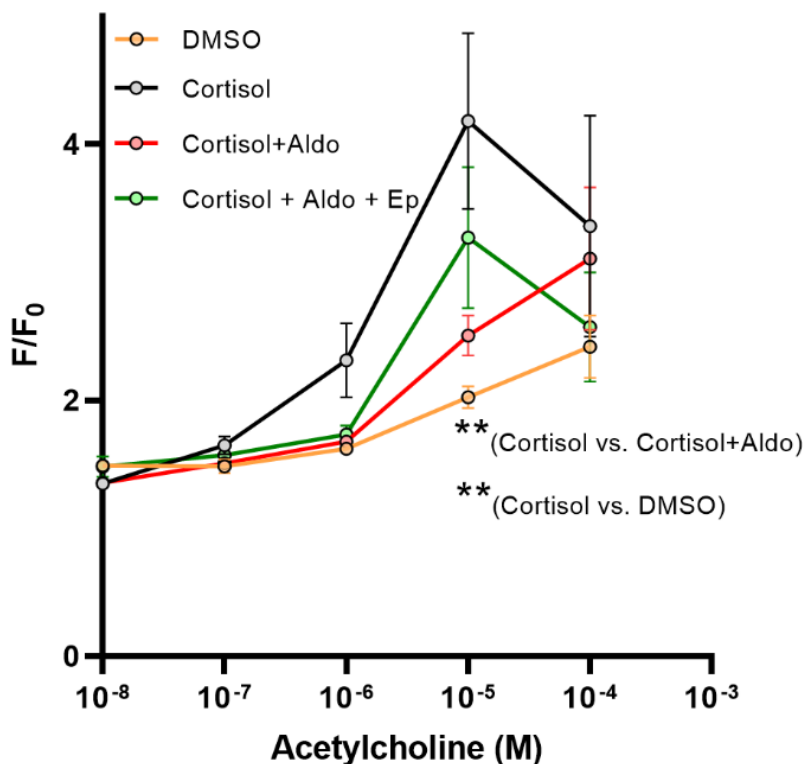


**Figure 7.** Calcium concentration-response curve for acetylcholine as determined by Fluo4 fluorescence in EC cultured for 48 hours in the presence of the indicated treatments. Aldo, 1  $\mu$ M aldosterone; Ep, 2  $\mu$ M eplerenone; N=6-11 measurements of at least 3 independent experi-

ments per group and concentration. \*\*, p<0.01 (Cortisol vs. Cortisol +Aldo and Cortisol vs. DMSO at 10  $\mu$ M acetylcholine). 2-Way ANOVA, Dunnett.

### 3.1.2 Quantification of stimulated EET release from endothelial cells

In order to address the question whether aldosterone has an impact on endothelial EET release, we treated endothelial cells for 48 hours and then acutely stimulated the release of EETs by adding either 1 or 100  $\mu$ M acetylcholine. These concentrations were chosen because they have been used in multiple prior studies in which they yielded submaximal to maximal effects in terms of vasodilation (Rand and Garland, 1992), calcium increase in endothelial cells in vascular preparations (Huang *et al.*, 2000) or calcium increase in cultured endothelial cells (Zuccolo *et al.*, 2019). EETs and DHETs were then quantified in the supernatants using HPLC MS/MS.

All eight eicosanoids (EETs and their diols) were detectable and quantifiable in the harvested supernatants. 14,15-EET and 14,15-DHET showed the highest concentrations. A summary of all concentrations in response to stimulation with 1  $\mu$ M acetylcholine is given in **Table 5**. **Table 6** provides the concentrations measured after stimulation with 100  $\mu$ M acetylcholine.

Eicosanoid release in EC in response to 1 $\mu$ M acetylcholine				
Treatment (n)	cortisol (6)	Aldo+cortisol (6)	Aldo+cortisol+Ep (6)	Aldo+cortisol +GSK (3)
<b>CYP epoxides (<math>\mu</math>mol/L)</b>				
5,6-EET	895,59 (195.28)	813,75 (174.80)	862,54 (196.68)	463,71 (114.39)
8,9-EET	623.81 (75.24)	678.44 (88.46)	636.24 (37.50)	628.16 (52.73)
11,12-EET	932.66 (74.05)	1048.26 (68.98)	946.66 (32.29)	<b>1214.07* (13.55)</b>
14,15-EET	1249.01 (77.63)	1344.54 (107.90)	1325.72 (45.51)	<b>1585.00<sup>§§</sup> (50.51)</b>
Sum EETs	3701.07 (407.61)	3884.98 (343.27)	3771.06 (249.70)	3890.93 (201.68)
<b>Epoxide hydrolase diols (<math>\mu</math>mol/L)</b>				
5,6-DHET	123.47 (21.06)	124.35 (30.70)	128.11 (30.67)	197.00 (15.39)
8,9-DHET	39.20 (5.33)	39.07 (3.99)	39.88 (5.28)	<b>55.48<sup>§</sup> (6.14)</b>

11,12-DHET	<b>257.89<sup>§§</sup> (48.71)</b>	236.34 (38.78)	<b>238.29<sup>§</sup> (37.92)</b>	<b>322.55<sup>§§§</sup> (26.59)</b>
14,15-DHET	<b>1022.22<sup>§</sup> (76.35)</b>	1071.35 (114.62)	1010.31 (110.12)	908.70 (78.48)
Sum DHETs	1442.79 (137.58)	1471.11 (183.89)	1416.58 (177.51)	1483.72 (122.84)
<b>CYP epoxygenase activity (μmol/L)</b>				
Sum EETs+DHETs	5143.86 (312.95)	5356.09 (331.30)	5187.65 (183.90)	5374.66 (228.38)
<b>Epoxide hydrolase activity (ratio)</b>				
5,6-DHET/EET	0.20 (0.07)	0.23 (0.09)	0.25 (0.10)	<b>0.49<sup>§§</sup> (0.15)</b>
8,9-DHET/EET	0.07 (0.01)	0.06 (0.01)	0.07 (0.01)	<b>0.09<sup>§</sup> (0.02)</b>
11,12-DHET/EET	<b>0.30<sup>§§</sup> (0.07)</b>	0.22 (0.03)	<b>0.25<sup>§</sup> (0.04)</b>	0.27 (0.02)
14,15-DHET/EET	<b>0.85<sup>§</sup> (0.10)</b>	0.81 (0.07)	0.76 (0.07)	0.57 (0.05)
Sum DHETs/sum EETs	<b>0.43<sup>§§§</sup> (0.08)</b>	<b>0.40<sup>§§</sup> (0.06)</b>	<b>0.39<sup>§§</sup> (0.07)</b>	<b>0.38<sup>§</sup> (0.04)</b>

**Table 5.** EET and DHET in EC supernatant after stimulation with 1 μM acetylcholine. Values as mean (SEM). Aldo, aldosterone 1 nM; DHET, dihydroxyeicosatrienoic acid; EC, endothelial cells; EET, epoxyeicosatrienoic acid; Ep, eplerenone 2 μM; GSK, GSK 2256294 3.3 nM. \*, p<0.05 vs. cortisol; 1-Way ANOVA, Dunnett. §p<0.05, §§p<0.01, §§§p<0.001 against the same treatment during culture and stimulation with 100 μM ACh, 1-way ANOVA, Šídák.

#### Eicosanoid release in EC in response to 100 μM acetylcholine

Treatment (n)	cortisol (9)	Aldo+cortisol (9)	Aldo+cortisol+Ep (9)	Al- do+cortisol+GSK
<b>CYP epoxides (μmol/L)</b>				
<b>5,6-EET (n=6)</b>	1082.37 (185.06)	1092.35 (148.07)	1051.58 (188.96)	1087.36 (207.49)
<b>8,9-EET</b>	819.42 (73.23)	874.76 (51.56)	847.54 (82.85)	836.27 (112.10)
<b>11,12-EET</b>	1123.84 (99.31)	1276.18 (60.67)	1230.42 (97.43)	1094.37 (117.02)
<b>14,15-EET</b>	1176.05 (43.30)	1336.27 (56.80)	1332.66 (80.86)	<b>1118.44 (70.95)<sup>§§</sup></b>

<b>Sum EETs (n=6)</b>	4562.05 (347.24)	4739.08 (244.50)	4622.17 (507.37)	4315.74 (553.67)
<b>Epoxide hydrolase diols (μmol/L)</b>				
<b>5,6-DHET</b>	144.97 (20.46)	165.29 (25.81)	154.59 (25.00)	120.58 (16.76)
<b>8,9-DHET</b>	32.89 (4.47)	38.36 (3.89)	35.14 (2.89)	<b>31.82 (3.47)§</b>
<b>11,12-DHET</b>	<b>129.51 (18.52)§§</b>	148.72 (19.02)	<b>136.82 (17.29)§</b>	<b>118.04 (14.55)§§§</b>
<b>14,15-DHET</b>	<b>625.44 (64.82)§</b>	713.11 (97.13)	678.06 (114.61)	506.72 (91.64)
<b>Sum DHETs</b>	932.80 (103.09)	1065.49 (144.39)	1004.60 (155.85)	777.16 (124.26)
<b>CYP epoxygenase activity (μmol/L)</b>				
<b>Sum EETs+DHETs (n=6)</b>	5306.73 (343.00)	5533.17 (231.04)	5330.06 (532.53)	4920.29 (602.65)
<b>Epoxide hydrolase activity (ratio)</b>				
<b>5,6-DHET/EET (n=6)</b>	0.12 (0.03)	0.12 (0.02)	0.12 (0.02)	<b>0.10 (0.02)§§</b>
<b>8,9-DHET/EET</b>	0.05 (0.01)	0.05 (0.01)	0.05 (0.01)	<b>0.04 (0.01)§</b>
<b>11,12-DHET/EET</b>	<b>0.13 (0.03)§§</b>	0.12 (0.02)	<b>0.12 (0.02)§</b>	0.12 (0.02)
<b>14,15-DHET/EET</b>	<b>0.55 (0.08)§</b>	0.54 (0.07)	0.51 (0.08)	0.45 (0.08)
<b>Sum DHETs/sum EETs (n=6)</b>	<b>0.17 (0.02)§§§</b>	<b>0.17 (0.02)§§</b>	<b>0.16 (0.01)§§</b>	<b>0.14 (0.01)§</b>

**Table 6.** EET and DHET in EC supernatant after stimulation with **100 μM** acetylcholine. Values as mean (SEM). Aldo, aldosterone 1 nM; DHET, dihydroxyeicosatrienoic acid; EC, endothelial cells; EET, epoxyeicosatrienoic acid; Ep, eplerenone 2 μM; GSK, GSK 2256294 3.3 nM. 1-Way ANOVA, Dunnett. §p<0.05, §§p<0.01, §§§p<0.001 against the same treatment during culture and stimulation with **1 μM** ACh, 1-way ANOVA, Šídák.

**Figure 8** provides a graphical overview and allows for a direct juxtaposition of the effects of both acetylcholine concentrations.

The following direct and derived measures were analyzed:

- individual concentrations of EETs and DHETs
- the sum of all EET and DHET concentrations to gauge overall EET production (CYP epoxygenase activity)
- individual DHET/EET concentration ratios to address regioisomer-selective degradation by preferential epoxide hydrolysis
- the sum of all four DHET/EET ratios as a measure of overall epoxide hydrolase activity

In summary, aldosterone+cortisol versus cortisol treatment did not result in significant changes in any of the described measures. Pre-treatment of cells with the soluble epoxide hydrolase

inhibitor GSK 2256294 (GSK) led to an increase in 11,12-EET concentrations compared to the control cells treated with cortisol.

While an obvious effect of aldosterone was absent, we, however, noted a striking acetylcholine concentration-dependent change in epoxide hydrolase activity: Supernatants from cells stimulated with 100  $\mu$ M acetylcholine showed significantly lower 11,12-DHET levels and lower sum of DHET/EET ratios than supernatants after 1  $\mu$ M acetylcholine. This effect was independent of the treatment preceding the acetylcholine stimulation. The sum of DHETs and EETs was unaltered, as were the concentrations of individual EETs. This indicated that the effect was mediated by acetylcholine-related inhibition of epoxide hydrolase activity, rather than a change in EET production.

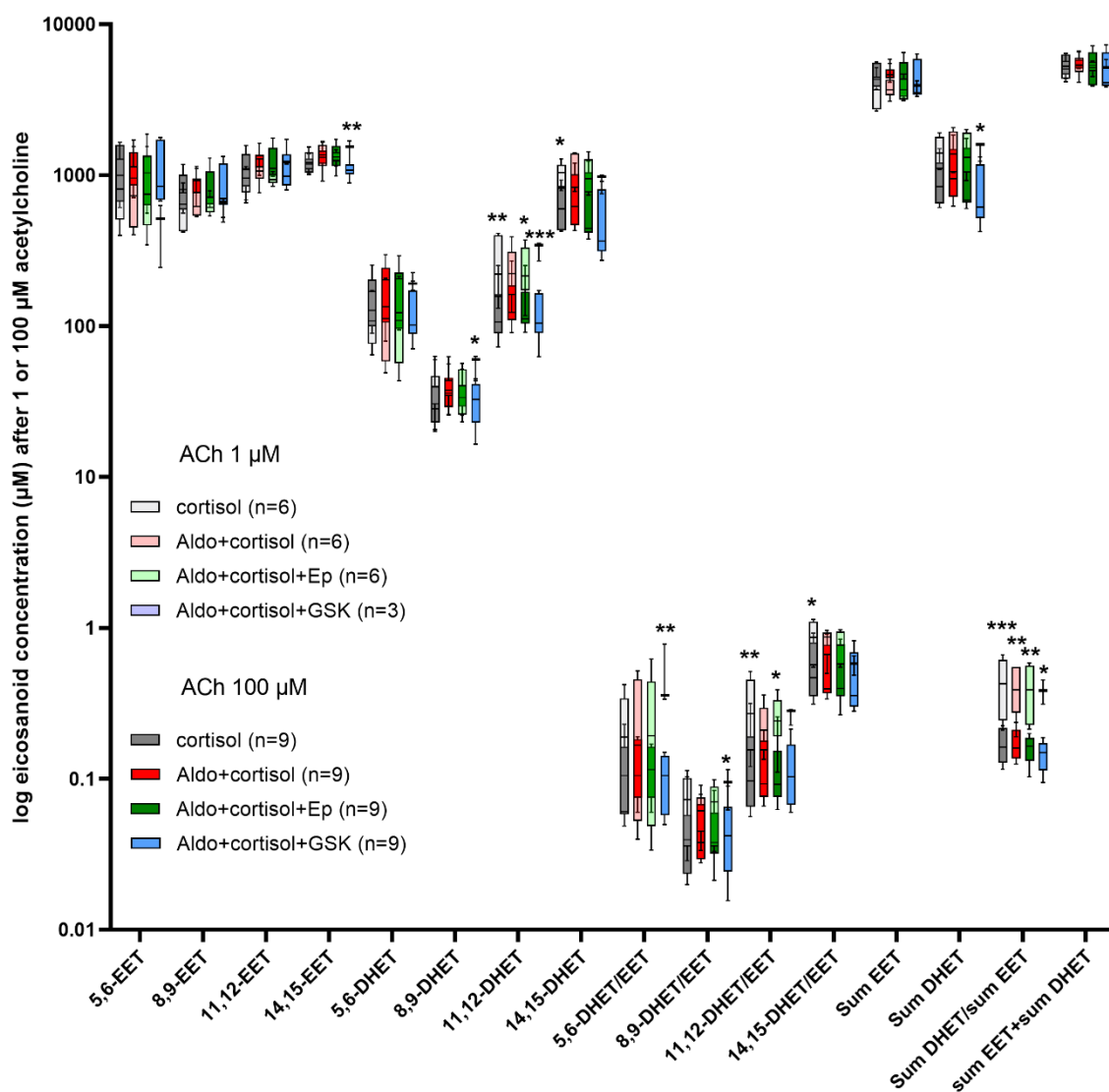


**Figure 8.** Overview of all EETs and DHETs and derived parameters in supernatants from endothelial cells after indicated treatments. Cells acutely stimulated with 1  $\mu$ M ACh are represented by box plots in **light colors**. Cells acutely stimulated with 100  $\mu$ M ACh are represented by **dark colors**. To compare acetylcholine concentration effects, cells who underwent identical culture conditions prior to stimulation but were simulated with different ACh concentrations are superimposed. Overlapping box plots indicate no effect of ACh concentration, separated box plots indicate ACh concentration-dependent effect. ACh, acetylcholine; Aldo, aldosterone; Ep, ep-

lerenone; GSK, GSK2256294. \*:  $p<0.05$ , \*\* $p<0.01$ , \*\*\* $p<0.001$  (ACh 1  $\mu$ M vs. 100  $\mu$ M), 1-way ANOVA, Šídák.

## 3.2 Part B: Cross-talk of endothelial glucocorticoid and mineralocorticoid receptors in aldosterone excess

### 3.2.1 Expression levels of endothelial 11 $\beta$ -hydroxysteroid dehydrogenases and their activities

The next project was designed to investigate the transcriptional responses of endothelial cells to glucocorticoids and mineralocorticoids, possible modulation of glucocorticoid response by mineralocorticoids and vice versa and mechanisms to assure selective stimulation of MR including steroid inactivating processes.

To this end, we started out determining the expression levels of 11- $\beta$ - hydroxysteroid dehydrogenase (HSD) type 1 and 11- $\beta$ -HSD type 2. The latter catalyzes the inactivation of cortisol to cortisone (with low affinity to mineralocorticoid receptors), the former catalyzes the reverse reaction (Chapman, Holmes and Seckl, 2013) (with cortisol bearing nearly identical MR affinity (Rupprecht *et al.*, 1993)).

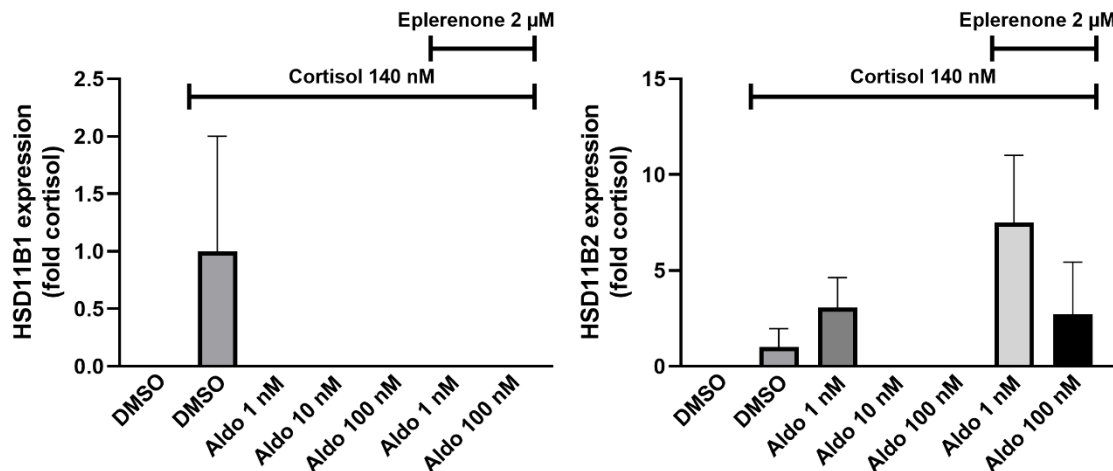


**Figure 9.** Relative mRNA expression levels of HSD11B1 (left) and HSD11B2 (right) in endothelial cells after 48 hours of indicated treatment. Shown are means of three independent replicates.

mRNA of both 11- $\beta$ -HSD type 1 and 11- $\beta$ -HSD type 2 could not be detected in most cases (**Figure 9**). An influence of cortisol or aldosterone on their expression levels could not be substantiated. Eplerenone induced HSD11B2 expression in some cells, although this increase was not statistically significant (either as tested by t-test versus DMSO control or Cortisol 140 nM + Aldo 1 nM). These findings raised the question whether endothelial cells were at all able to protect their mineralocorticoid receptors from circulating cortisol.

To assess relative 11- $\beta$ -HSD type 1 and 11- $\beta$ -HSD type 2 activity, we measured cortisol and cortisone in supernatants of endothelial cells after 48 hours of treatment. In parallel, we also determined aldosterone concentrations to detect any metabolism of aldosterone as a function of cell treatment. Treatments comprised an exposure to 1 nM, 10 nM and 100 nM aldosterone (all with parallel application of 140 nM cortisol) and the same concentrations of aldosterone in the presence of 2  $\mu$ M eplerenone. This was compared to 140 nM cortisol alone and a solvent (DMSO) control. All post-treatment steroid concentrations in endothelial supernatants can be found in **Table 7**.

We consistently registered higher actual cortisol concentrations than the intended concentration of 140 nM across all treatments which involved 140 nM cortisol. This, however, also applied to endothelial cell medium freshly spiked with 140 nM cortisol and 1 nM aldosterone which had not been in contact with cells. In this medium we measured mean cortisol concentrations of  $245.8 \pm 11.6$  nM. It is, thus, fair to assume higher than intended cortisol stock concentrations (1.8 times higher concentration) rather than cortisol production in endothelial cells. Cortisol, on the other hand, was measurable in medium from DMSO-treated cells, which may indicate a minor contribution of endothelial steroid production to overall concentration (**Figure 10A**).

All supernatants which contained steroids showed low levels of cortisone. These levels were always below the lower limit of quantification (LOQ). We decided to quantify the results by using the actually measured concentrations, even if they were below the LOQ, because replacing the measured values by the numerical value of the LOQ would have introduced a false uniformity (**Figure 10B**).

Aldosterone stocks, on the other hand, were obviously lower concentrated than intended (mean  $0.658 \pm 0.015$  nM, 0.685 times lower concentration). As a note of caution the stocks used to spike endothelial cell medium were not the same as the stocks used to generate the cell culture supernatants, so the actual deviation of stock concentrations is unknown. There were no hints to baseline aldosterone production in endothelial cells, as supernatants from this group had undetectable aldosterone levels (**Figure 10D**).

Aldosterone in a range of 1 to 100 nM did not alter the supernatant cortisol concentration. Neither did antagonization of the mineralocorticoid receptor result in differences when compared to the control (being hydrocortisone 140 nM treatment) (**Figure 10A**).

We did detect an impact of treatment with aldosterone 10 nM plus hydrocortisone when compared to hydrocortisone alone: This led to a significant increase in supernatant cortisone, an effect that was not remediable by eplerenone. To our surprise this effect did not show a concentration-dependence (**Figure 10B**). Following the aforementioned changes in cortisone, the cortisol/cortisone ratio was decreased in supernatants from cells treated with hydrocortisone plus aldosterone 10 nM  $\pm$  eplerenone, formally indicating increased 11- $\beta$ -HSD type 2 activity in these groups (**Figure 10C**).

Antagonization of 100 nM aldosterone with eplerenone led to a slight but significant decrease in aldosterone supernatant concentration when compared to the unopposed stimulation with 100 nM.

At high concentrations of aldosterone, adding eplerenone significantly reduced the measurable aldosterone concentration, which may indicate metabolism of aldosterone (**Figure 10D**).

In summary, endothelial cells did demonstrate cortisone production when challenged with cortisol, indicating 11- $\beta$ -HSD type 2 activity. Aldosterone did not show a concentration-related effect

on 11- $\beta$ -HSD type 2 activity. Endothelial cortisol synthesis is negligible. No signals for aldosterone synthesis originating from endothelial cells could be detected.

---

**Steroid concentrations (nmol/L) after indicated treatment**

---

Treatment (n)	Cortisol	Cortisone	Cortisol/cortisone	Aldosterone
<b>DMSO (3)</b>	2.2 (0.7)	0.000 (0.000)	-	0.000 (0.000)
<b>Cortisol (9)</b>	194.9 (4.3)	0.176 (0.006)	1125 (55.6)	0.000 (0.000)
<b>Cortisol+ Aldo 1 nM (9)</b>	194.4 (2.9)	0.182 (0.009)	1087 (53.0)	0.871 (0.060)
<b>Cortisol+ Aldo 10 nM (6)</b>	193.9 (5.0)	0.257 (0.022)	794.3 (91.6)	10.350 (0.431)
<b>Cortisol+ Aldo 100 nM (6)</b>	194.8 (4.7)	0.220 (0.022)	931.6 (95.9)	102.400 (2.544)
<b>Cortisol+ Aldo 1 nM + Ep 2 <math>\mu</math>M (6)</b>	201.6 (2.0)	0.163 (0.009)	1253 (72.0)	0.983 (0.014)
<b>Cortisol+ Aldo 10 nM + Ep 2 <math>\mu</math>M (3)</b>	188.3 (4.2)	0.307 (0.009)	615.8 (30.8)	11.160 (0.275)
<b>Cortisol+ Aldo 100 nM + Ep 2 <math>\mu</math>M (3)</b>	198.5 (1.9)	0.157 (0.007)	1272.0 (59.2)	95.450 (3.733)
<b>Medium + Cortisol + Aldo 1 nM without cell contact (2)</b>	245.8 (11.6)	0.195 (0.135)	2499.4 (1789.8)	0.685 (0.015)

**Table 7.** Concentrations of indicated steroids as determined by LC-MS/MS in endothelial cell culture supernatants harvested after 48 hours of specific treatment. Values as mean (SEM). Aldo, aldosterone; Ep, eplerenone. Number of replicates is provided in parentheses in the treatment column.

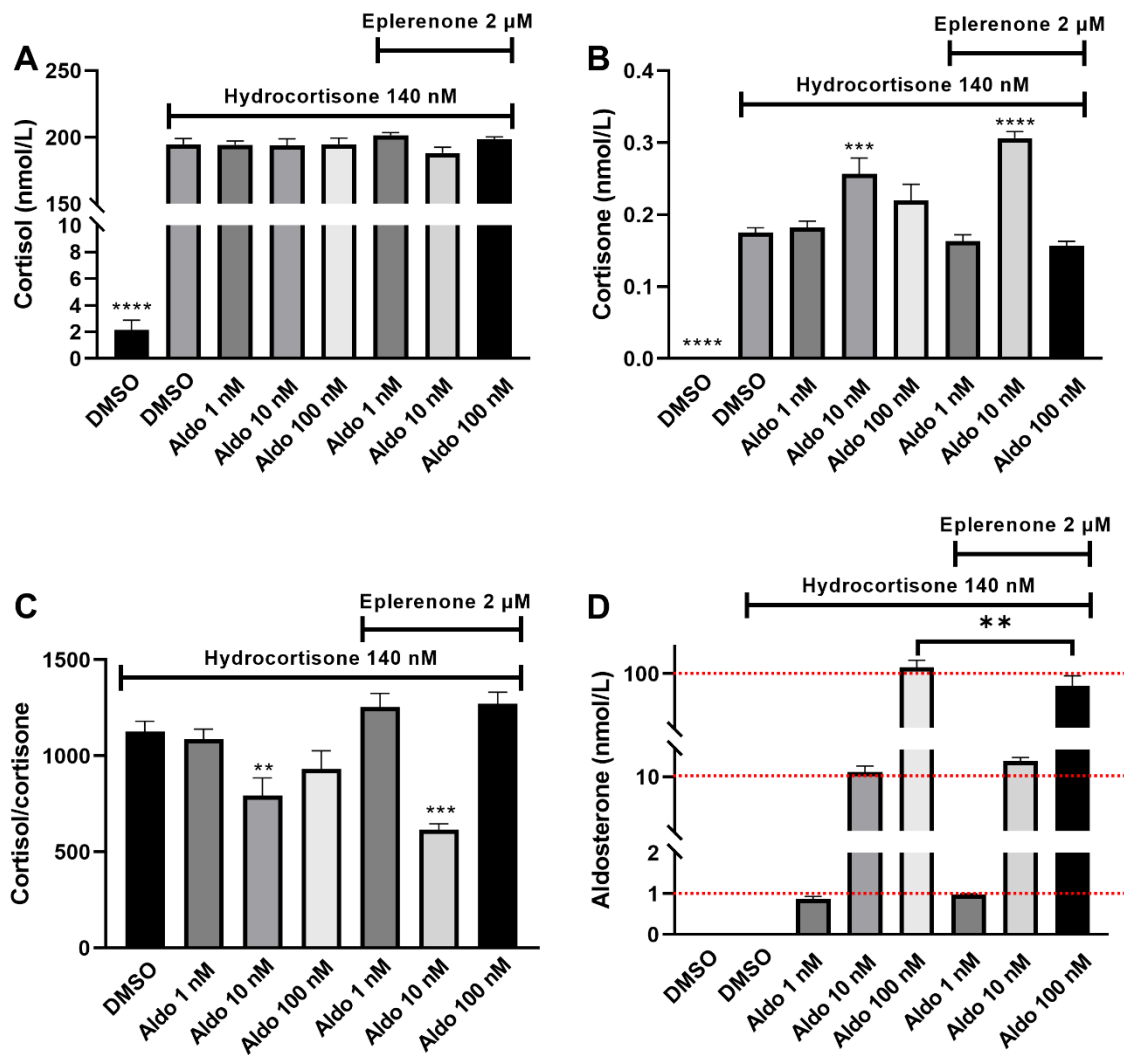


**Figure 10.** Steroids in supernatants of endothelial cells after 48 hours of treatment. **A**, cortisol; \*\*\*\* p<0.0001 versus Hydrocortisone + DMSO, 1-Way ANOVA, Dunnett. **B**, cortisone; \*\*\* p<0.001, \*\*\*\*p<0.0001 versus Hydrocortisone + DMSO, 1-Way ANOVA, Dunnett. **C**, cortisol/cortisone ratio; \*\* p<0.01, \*\*\*p<0.001 versus Hydrocortisone + DMSO, 1-Way ANOVA, Dunnett.; **D**, aldosterone; \*\*p<0.01, Aldo 100 nM + hydrocortisone versus Aldo100 nM + hydrocortisone + eplerenone, 1-Way ANOVA, Sidak. Red dotted line indicates intended aldosterone concentrations to delineate possible effects of eplerenone versus the unantagonized stimulation. All concentrations in nmol/L. n=3-9 independent replicates per treatment. Values as means  $\pm$  SEM.

### 3.2.2 MR and GR marker gene transcription and interaction

We used FKBP5 as marker gene for GR-mediated transcriptional activity (Vermeer *et al.*, 2003). With respect to DMSO-treated cells we could not detect significant increases in FKBP5 transcription in response stimulation with 140 nM hydrocortisone (Figure 11, left). Aldosterone likewise did not induce significant changes. The only significant changes we saw were an increase in FKBP5 mRNA in cortisol, aldosterone and eplerenone co-treated samples. Although FKBP5 message increased numerically in response to cortisol treatment, this effect did not reach statistical significance. This assay, thus, does not permit to draw conclusions on the transactivation of MR and GR by aldosterone and hydrocortisone treatment.

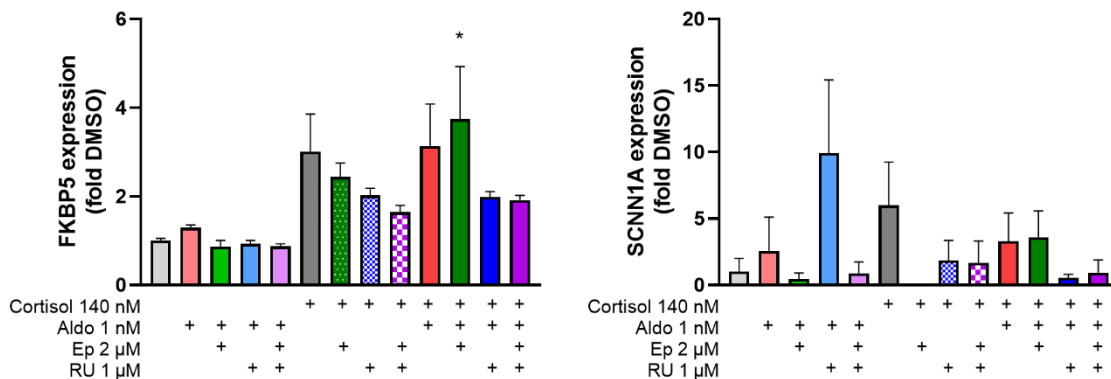


**Figure 11.** Expression levels of the GR marker gene FKBP5 (left) and the MR marker gene SCNN1A (right) in response to isolated and combined mineralocorticoid and glucocorticoid application and respective antagonization. N=3-6 independent replicates per treatment. \*p<0.05 versus DMSO treatment, 1-Way-ANOVA, Dunnett's.

Using higher aldosterone concentrations with concomitant cortisol stimulation, we tried to unmask an interaction between GR and MR agonists. Again, no statistically significant effects were found **Figure 12**, left). Trends suggested a dose-dependent reduction in FKBP5 transcription but conclusions were hampered mostly by larger errors.

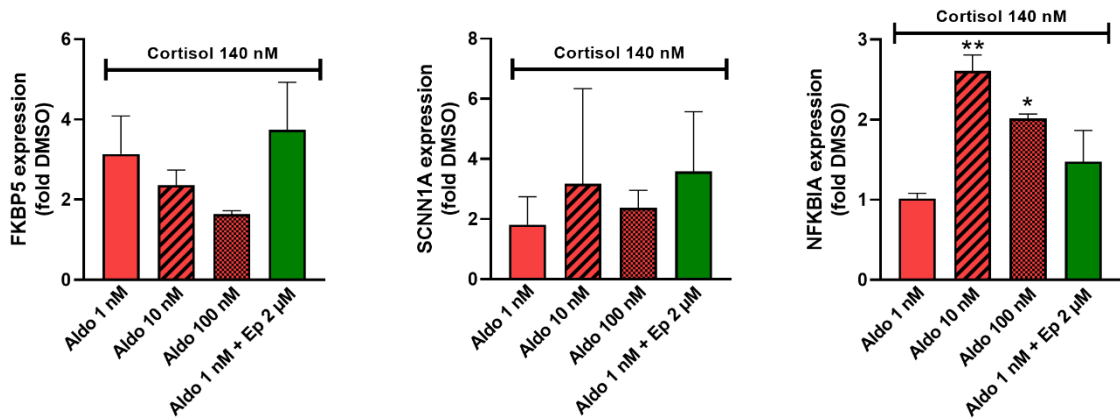


**Figure 12.** Aldosterone concentration-response curve, GR marker gene FKBP5 (Left), MR marker gene SCNN1A (middle), putative MR marker gene NFKBIA (right). Values as means  $\pm$  SEM. n=3 independent replicates per treatment. 1-Way ANOVA, Dunnett. \*p<0.05 versus Aldo 1 nM + cortisol, \*\*, p<0.01 versus Aldo 1 nM + cortisol.

Finding a qPCR assay which was able to demonstrate MR transcriptional activity turned out even harder due to the low abundance in classical target expression such as SCNN1A (the gene coding for ENaC channel alpha subunit).

We could not demonstrate that SCNN1A message in endothelial cells is regulated by stimulation with physiological concentrations of either aldosterone or hydrocortisone **Figure 11**, right). Likewise, higher concentrations of aldosterone did not result in significant changes in SCNN1A expression (**Figure 12**, middle).

Data mining of publicly available RNAseq data from endothelial cells (HUVEC) treated with 100 nM aldosterone (Moser *et al.*, 2018) performed in our group previously had shown that aldosterone induced a MR-dependent 1.3 fold increase in NFKBIA expression (the gene coding for

nuclear factor  $\kappa$ B (NF $\kappa$ B) inhibitor  $\alpha$ ). We, therefore, chose to investigate NFKBIA as novel marker of MR transcriptional activity.

Changes in NFKBIA transcript levels could be detected from 10 nM aldosterone onwards, demonstrating that our cell culture system was able to detect MR-related expression changes (**Figure 12**, right). Physiological concentrations of aldosterone (1 nM), however, did not result in significant increases when compared to the DMSO control. In addition, NFKBIA expression changes required the presence of cortisol and were not apparent in cells only exposed to aldosterone.

### 3.2.3 Semiquantitative parallel analysis of MR and GR activation by immunofluorescence

Endothelial cells were cultured under indicated treatment conditions for 48 hours on immunofluorescence-compatible slides, fixed, permeabilized and stained with antibodies directed against the glucocorticoid and the mineralocorticoid receptor. In addition, nuclei were visualized using DAPI. The DAPI-positive areas were outlined and defined as regions of interest (ROI). Then, fluorescence signal intensities of GR and MR in the same ROIs were determined.

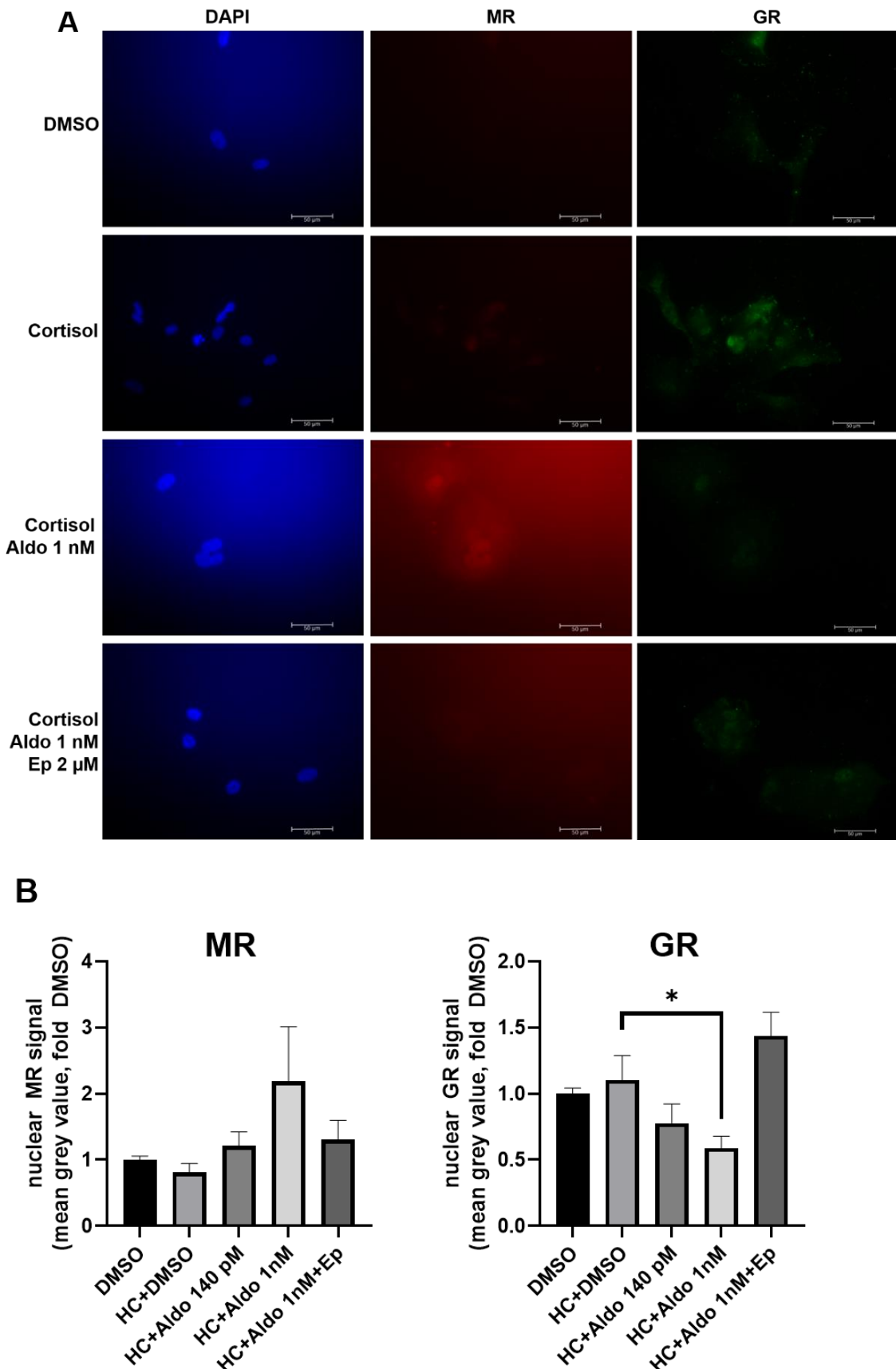


**Figure 13.** A, original immunofluorescence images of four different treatment conditions (DMSO, 140 nM cortisol, 140 nM cortisol + 1 nM aldosterone, 140 nM cortisol + 1 nM aldosterone + 2  $\mu$ M epplerenone with nuclear DAPI signal in blue (left column), MR signal in red (middle

column) and GR signal in green (right column). Images were not digitally manipulated and are presented as they were recorded. White scale bars 50  $\mu$ m. **B**, summary of mean grey values for MR and GR in the nuclear ROIs. n= 9 different analyses from 3 independent replicates per treatment group. \*p<0.05, 1-Way ANOVA, Dunnett. DAPI, 4',6-diamidino-2-phenylindole. MR, mineralocorticoid receptor, GR, glucocorticoid receptor.

The results were interesting in so far that we saw an aldosterone-dependent tendency of an increase in nuclear MR signal. Eplerenone treatment reduced the nuclear signal again. Both effects were, however, not statistically significant (**Figure 13A, middle row, 13B, left**).

When the nuclear GR signal was examined, we observed a diffusely scattered signal of GR aggregated throughout the cytoplasm in solvent-treated cells. In cells treated with cortisol, these aggregated became somewhat more concentrated in the area of the nucleus. Moreover, steroid-treated cells featured GR-positive ring-like structures in the DAPI-marked ROIs. These ring-like structures were only rarely present in DMSO-treated cells and never in those in which the primary staining antibody had been omitted.

Aldosterone led to a concentration-dependent decrease in nuclear abundance of GR. This effect could be inhibited by eplerenone, indicating an MR-related process. Of note, only the excess concentration, 1 nmol/L, significantly reduced the nuclear GR signal. Physiological levels of 140 pmol/L did not result in a significant decrease (**Figure 13A right row, 13B, right**).

## 4. Discussion

### 4.1 Part A

#### 4.1.1 Gene expression levels

In the experiments of chapter A, the goal was to test the hypothesis that aldosterone might disturb endothelial function by impairing the EET pathway. Primary human coronary artery endothelial cells were used because of evidence in the literature that in this vascular territory the EET pathway is functionally important (Larsen *et al.*, 2006) and because of the immediate implications of potential findings to the pathophysiology of coronary artery disease. Across species, EETs also were reported to regulate tone in bovine coronary arteries (Gauthier *et al.*, 2002, 2005).

Care was taken to approximate *in vivo* conditions as far as possible: We employed cortisol concentrations of 140 nM which can be measured in human serum both in the morning as well as in the evening (Van Cauter, Leproult and Kupfer, 1996). Aldosterone concentrations of 1 nM were chosen similar to the third quartile of plasma aldosterone concentration in patients with PA (0.794 nM) as published in the most recent overview of the Munich Conn's registry (Heinrich *et al.*, 2018). To exclude effects of other steroids contained in fetal calf serum, cells were serum-deprived prior to stimulation and stimulation was carried out in serum-free medium.

The steroid concentrations were effective in that they induced the expression of a mesenchymal marker gene in endothelial cells and impaired endothelial calcium response to acetylcholine (see below).

This study is the first to report evidence on possible endothelial to mesenchymal transition in the context of aldosterone excess. Provided our finding can be further substantiated by assessing other phenotype markers, the results would have significant impact on the concept of aldosterone-mediated endothelial dysfunction and should then entail further investigation to delineate the underlying mechanisms.

We detected low but quantifiable mRNA levels of both CYP2J2 and CYP2C8 in coronary artery endothelial cells. CYP2C9 was not detected. DeLozier and colleagues measured all 3 CYP epoxygenases in five different human coronary artery extracts by qPCR and western blot. In addition, they assessed two human heart samples with immunohistochemistry. They found low and consistent CYP2C8 expression, and higher but more variable levels of CYP2J2 as well as CYP2C9. Protein was detected for CYP2C9 and CYP2J2 only, with CYP2C9 being more abundant. On the contrary, immunohistochemistry could only demonstrate CYP2J2 and CYP2C8 in endothelial cells. The authors concluded that CYP2C9 is the most abundant epoxygenase in coronary arteries (DeLozier *et al.*, 2007). These results are in conflict with our findings. One explanation for this may be the fact that most of the tissue samples were from patients with some degree of atherosclerotic disease. In another study which used plasma concentrations of patients with coronary artery disease, the disease extent was negatively correlated with CYP2J2 expression levels in peripheral blood mononuclear cells, suggesting that atherosclerosis may modulate CYP epoxygenase expression levels (Oni-Orisan *et al.*, 2016).

We could not find any published data which address an impact of aldosterone on the expression levels of the three epoxygenases, so external validation of these results was not possible.

Reports directly addressing the expression of epoxide hydrolases in endothelial cells are rare. In mouse brains, Marowsky and co-workers described only mEH immunofluorescence in brain microvascular endothelial cells. Expression of sEH was confined to astrocytes and not reported for endothelial cells (Marowsky *et al.*, 2009). These findings were further extended by Gupta *et al.* who showed that murine male endothelial cells had greater Ephx2 expression levels than female cells. This increased baseline expression in males translated to an abrogated decrease in Ephx2 mRNA which was seen in females in response to oxygen and glucose deprivation (Gupta *et al.*, 2012).

Okada and co-workers on the other hand, could show that rat aortic endothelial cells feature baseline expression of soluble epoxide hydrolase (Okada *et al.*, 2017). sEH was also detected in primary lung endothelial cells by Deng and co-workers (Deng *et al.*, 2011).

In human umbilical vein endothelial cells (HUVEC), expression of functional mEH was detected, suggesting that this enzyme might play a role in vascular physiology beyond the arterial system (Farin, Pohlman and Omiecinski, 1994).

Edin *et al.* provide indirect evidence of both epoxide hydrolases being present in cardiac tissue. They examined cardiac perfusates obtained from knock out mice for Ephx1, Ephx2 or both enzymes in postischemic reperfusion. Baseline levels of 14,15-DHET and 11,12-DHET were reduced at baseline and after ischemia only in the dual gene-deficient mice. These findings indicate a mutual compensation of both epoxide hydrolases in case of functional loss of either Ephx1 or Ephx2. However, the nature of the cells expressing Ephx1 and Ephx2 remained undetermined (Edin *et al.*, 2018).

Studies addressing microsomal epoxide hydrolase expression in endothelial cells could not be found.

Of note, a liver-specific expression of EPHX1 alternative exon 1b has been reported, whereas the other tissues examined (including cardiac tissue) featured the conventional exon 1 (Liang, Hassett and Omiecinski, 2005). Our gene expression assay was designed as an intron-spanning assay further downstream of exon 1, thereby precluding any interference of alternative exons with gene expression analysis.

The impact of aldosterone on epoxide hydrolase activity was only investigated in one study: An increase in mouse adipose tissue Ephx2 expression in response to aldosterone infusion was reported by Luther and colleagues (Luther *et al.*, 2021).

Using the mineralocorticoid precursor deoxycorticosterone acetate plus salt administration (DOCA-salt) in mice, Lee *et al.* could not detect changes in sEH protein levels in kidney tissue (Lee *et al.*, 2011).

In sum, our findings that coronary artery endothelial cells express both EPHX1 and EPHX2 seem to be in line with the findings of other studies addressing the expression levels in other vascular territories. Effects of *in vivo* pathological concentrations of aldosterone on epoxide hydrolase expression levels in endothelial cells still remain to be determined.

### 4.1.2 Calcium response in endothelial cells

In our studies we observed that pre-treatment with physiological cortisol concentrations enhances the calcium influx to acetylcholine when compared to cells treated only with solvent. The sole publication to also address the effects of preceding exposure to glucocorticoids on the endothelial calcium response used very high cortisol concentrations (1  $\mu$ M) in endothelial cells and observed the opposite, e.g. that ATP-mediated calcium increase was reduced in the cortisol-treated cells (Rogers *et al.*, 2002). The explanation for this difference probably lies in the effects of physiological versus pathological cortisol concentrations.

We further demonstrated that aldosterone impaired the endothelial calcium response to acetylcholine.

Despite acetylcholine having been used in a myriad of studies addressing the physiology in isolated vessels, we are unaware of other publications which used the cytosolic calcium increase in response to acetylcholine as a measure of endothelial dysfunction, i.e. in investigations related to pathophysiology. Early studies confirmed the endothelial calcium increase by acetylcholine (Busse *et al.*, 1988; Falcone, Kuo and Meininger, 1993) and a publication of Huang and colleagues demonstrated a calcium concentration-response curve for endothelial cells (Huang *et al.*, 2000).

We noted a concentration-dependent increase in endothelial cytosolic calcium up to concentrations of 10  $\mu$ M. Then the calcium signal became more variable which resulted in a mean decrease at the maximum concentration of 100  $\mu$ M.

Huang and colleagues also demonstrated a peak calcium response at 10  $\mu$ M acetylcholine in endothelial cells labelled *in situ* in vascular preparations. Concentrations beyond 100  $\mu$ M were not examined (Huang *et al.*, 2000). Of note, Zuccolo *et al.* described that ACh 100  $\mu$ M elicited a maximal calcium increase whereas the calcium in response to 300  $\mu$ M dropped again. One hypothetical explanation for this disconnect at high concentrations might be receptor arrestin-mediated receptor sequestration which is known to occur with muscarinic acetylcholine receptors (Vögler *et al.*, 1999; Luo, Busillo and Benovic, 2008).

Our experiments do not allow to draw conclusions about the aldosterone-sensitive structure which mediates calcium influx in endothelial cells.

Concepts of acetylcholine-mediated calcium increase in endothelial cells suggest that acetylcholine binds to and activates muscarinic M3 or M5 acetylcholine receptors (Zuccolo *et al.*, 2017, 2019). Subsequently, G<sub>q/11</sub> proteins are activated, dissociate and induce activation of phospholipase C. This then results in the generation of diacylglycerol and IP<sub>3</sub> (Caulfield and Birdsall, 1998). DAG can theoretically activate TRPC channels but this has been shown to be not the case for muscarinic M3 receptors in mouse brain endothelial cells (Zuccolo *et al.*, 2017). The other second messenger, IP<sub>3</sub>, is supposed to bind to IP<sub>3</sub> receptors on the endoplasmic reticulum, which leads to the release of calcium from this internal store as pulsars in close proximity to underlying smooth muscle cells (Ledoux *et al.*, 2008). These pulsars in turn lead to endothelial hyperpolarization by opening of SK<sub>Ca</sub> and IK<sub>Ca</sub> channels, hyperpolarization of underlying smooth muscle and to, ultimately, vasodilation (Ottolini, Hong and Sonkusare, 2019). It has also been reported that muscarinic acetylcholine receptor activation in endothelial cells couples to TRPV4 channel activation. These channels then trigger calcium influx (called sparklets) which then activate SK<sub>Ca</sub> and IK<sub>Ca</sub> channels (Sonkusare *et al.*, 2012). Of note, endothelial TRPV4 channels can also be activated via low transmural pressure, indicating a role in the autoregulation of tissue perfusion (Bagher *et al.*, 2012).

Ryanodine receptors, which can also release calcium from the endoplasmic reticulum, were not detected in mouse brain endothelial cells (Zuccolo *et al.*, 2017) but in freshly isolated human mesenteric artery endothelial cells (Köhler *et al.*, 2001). Köhler and colleagues also demonstrated their functional integrity by caffeine-mediated hyperpolarization (Köhler *et al.*, 2001).

Future studies should investigate the expression of each of the aforementioned structures, starting from acetylcholine receptors to IP<sub>3</sub> receptors and SK<sub>Ca</sub> and IK<sub>Ca</sub> channels to determine whether differences in protein levels can account for the observed diminished acetylcholine response. Approaches using next generation sequencing and clustering of transcripts by appropriate gene ontology terms might facilitate the discovery of aldosterone-induced expression changes. These experiments should be followed by pharmacological and genetic manipulation to unravel the functional role of any dysregulated proteins.

#### 4.1.3 Stimulated EET release by endothelial cells

In endothelial cells pre-treated with aldosterone we could not detect differences in stimulated EET release.

Liu and colleagues described that patients with primary aldosteronism showed increased serum levels of 14,15-DHET. Levels of 14,15-DHET were positively correlated with plasma aldosterone concentrations and calcification scores of the abdominal aorta (Liu *et al.*, 2018). We were not able to reproduce this finding in endothelial cell supernatants, possibly for the following reasons: Lui *et al.* used an ELISA method to quantify 14,15-DHET, so the two different analytical methods may have produced different results. Further, Liu and colleagues used circulating EETs as proxy for endothelium-derived EETs. It should be stated that, however, other cells such as red blood cells may synthesize and release EETs, which could substantially obscure any conclusions about the cellular origin of circulating eicosanoids (Jiang, Anderson and McGiff, 2010).

The other study in which EETs were analysed in the context of PA used plasma EETs from patients with PA before and after therapy. While they could not detect differences in 14,15-DHET, they described an increase in the sum of all EETs and of 14,15-EET in particular. 5,6-EET was not measured, so the sum of EETs here only included three regioisomers. Plasma aldosterone concentrations also correlated inversely with concentrations of 11,12-EET, 14,15-EET and the sum of EETs. This study suggested that recovery from PA goes along with increases in plasma EETs. However, because the study lacked a true control group it is unclear whether these changes represent a reversal of aldosterone-induced changes at baseline (Luther *et al.*, 2021). An alternative explanation might, thus, be that PA therapy was the confounder which both modulated aldosterone and plasma EETs. Further and larger studies should be conducted to truly affirm a causal role of aldosterone on circulating eicosanoids. Again, the above-mentioned differences between circulating EETs and EETs directly harvested from cultured endothelial cells may account for the fact that we did not observe aldosterone-mediated changes.

In general, the pattern of EETs secreted by our endothelial cells has been described by other groups: Using the same cell type as in our experiments, Zheng and coworkers described that these cells release also mainly 14,15-EET upon stimulation with arachidonic acid (Zheng *et al.*, 2013). This is in agreement with Fisslthaler *et al.* who reported that porcine coronary artery endothelial cells synthesize preferentially 11,12-EET and 14,15-EET in response to stimulation with cyclic strain (Fisslthaler *et al.*, 2001). However, they did not analyze supernatants but used

whole cell extracts, which likely captured significant amounts of intracellular EETs esterified to phospholipids. 25 % of the total 14,15-EET pool in endothelial cells are estimated to be stored as phospholipids and are not released upon stimulation (Fang, Weintraub and Spector, 2003).

Bovine endothelial cells also were described to synthesize mainly 14,15-EET in response to stimulation with the acetylcholine-like compound methacholine. Again, they used whole cell extracts. Other EET regioisomers were detectable but not quantifiable due to their low concentration (Nithipatikom, Pratt and Campbell, 2000).

11,12-EET and 14,15-EET were also detected in the perfusate from a single cannulated bovine coronary artery and increased in response to stimulation with bradykinin. Other EETs were not reported. No EETs were detected in endothelium-denuded arteries (Gauthier *et al.*, 2005).

The sum of EETs and DHETs was unaltered between cells stimulated with 1 or 100  $\mu$ M ACh whereas the DHET/EET ratio was significantly increased in 1  $\mu$ M-stimulated cells. We interpret these findings in line with the hypothesis of a release of preformed, phospholipid-bound EETs rather than de novo synthesis (Spector *et al.*, 2004). These findings would also be more compatible with the low mRNA expression levels of CYP epoxygenases, which would make a de novo synthesis upon activation an unlikely scenario in these endothelial cells.

Cells cultured in the presence of the sEH inhibitor GSK still showed significant differences in the DHET/EET ratios between the two acetylcholine stimulations. This finding may indicate that acetylcholine inhibits mEH rather than sEH. One potential mechanism for this may be the fact that human mEH has been shown to experience roughly 20 % reduction in activity upon exposure to calcium (and other metals) (Draper and Hammock, 1999). The acetylcholine-induced calcium increase may, thus, facilitate the release of preformed EETs by inhibition of otherwise tonic mEH activity. Further studies in this direction are warranted.

As a note of caution, in our experiments the soluble epoxide hydrolase inhibitor GSK was present during the preceding 48 hours of culture, prior to the actual stimulation. During stimulation we did not include GSK. Soluble epoxide hydrolase function may, thus, have recovered in the time after removal of culture medium. Still, 11,12-EET concentrations were higher in supernatants from GSK-pretreated, 1  $\mu$ M acetylcholine-stimulated cells than in control cells, indicating that GSK at least for this eicosanoid showed efficacy. Because pretreatment with GSK did not result in a parallel reduction of 11,12-DHET one may speculate that the excess 11,12-EET may have gradually accumulated over time via incorporation in membrane phospholipids, a stock that was then released upon stimulation with acetylcholine, rather than acute de novo formation.

Our final conclusion from chapter A was that EETs are produced and degraded normally in aldosterone excess.

## 4.2 Part B

### 4.2.1 Expression levels of endothelial 11 $\beta$ -hydroxysteroid dehydrogenases and their activities

While chapter A investigated changes in endothelial cells inflicted by steroid excess, chapter B focused on changes in steroid concentrations by means of endothelial enzymes and steroid receptor transactivation.

A primary finding of our study was that human coronary artery endothelial cells do not express 11- $\beta$ -HSD type 1 or 11- $\beta$ -HSD type 2 mRNA. Neither did measurements of cortisone reveal a significant HSD11B2 activity since cortisol levels after 48 hours were usually still in excess of cortisone concentrations by a factor of 1000.

We were surprised to see that 140 nM of cortisol also only inconsistently induced HSD11B since in a lot of tissue types, glucocorticoids are reported to actually increase HSD11B1 expression (Chapman, Holmes and Seckl, 2013). While Liu and coworkers could detect both HSD isoforms in human umbilical vein endothelial cells (HUVEC), they also noted that treatment with cortisol did not change their expression levels. HSD11B1 and HSD11B2 in endothelial cells, thus, do not seem to be under the transcriptional control of glucocorticoids (Liu *et al.*, 2009).

Brem and colleagues also demonstrated the presence of 11- $\beta$ -HSD type 1 in HUVEC, whilst 11- $\beta$ -HSD type 2 could not be detected. The two 11- $\beta$ -HSD types were regulated in a reciprocal manner. Factors which decreased 11- $\beta$ -HSD type 1 were a reduction of the serum concentration in cell culture medium, and when cells reached a high confluence of 95 % (as compared to 60 % confluence). Adding a scratch wound as a regenerative stimulus increased 11- $\beta$ -HSD type 1 expression (Gong, Morris and Brem, 2008). One reason that in our hand we could barely detect both mRNA levels of both 11- $\beta$ -HSD types may be that cell underwent complete serum starvation for a total period of 56 hours before and whilst undergoing steroid exposure. This complete deprivation may have reduced the expression levels to nearly zero. Other factors may have been that our cultured cells originated from different vascular territory and type (coronary artery versus umbilical vein) and, hence, may harbor inherently different properties as compared to those used by Brem and coworkers.

The same group showed in rat aortic endothelial cells a predominantly 11- $\beta$ -HSD type 1 activity which resulted in the conversion of up to 15 % of 11-Dehydrocorticosterone to corticosterone. 11- $\beta$ -HSD type 2 activity resulted in only a few % conversion of corticosterone to 11-Dehydrocorticosterone (Brem *et al.*, 1998). Our results are in agreement with these findings concerning that 11- $\beta$ -HSD type 2 activity is low. Numerically we arrive at much lower 11- $\beta$ -HSD type 2 activities of <1% conversion (cortisol usually being 600 to 1200-fold higher concentrated than cortisone).

We assume that the cortisol concentration in spiked medium can be taken as the starting concentrations before the 48 hours culture period. The starting concentration, therefore, was  $245.8 \pm 11.6$  nM. The mean concentration of all supernatants after 48 hours was  $195.2 \pm 1.6$  nM. When cortisone concentrations (assuming that these represent exclusively daughter metabolites of cortisol) are added to the cortisol levels one arrives at concentrations of  $195.4 \pm 1.5$  nM, still a substantial difference to the spiked medium. This raises the question whether cortisol and/or cortisone are metabolized to further daughter substances which were not measured in our assay. Cortisone can be further converted to tetrahydrocortisone by 5 $\beta$ -reductase and 3 $\alpha$ -hydroxysteroid dehydrogenase. Also, cortisol may be inactivated to other metabolites than cortisone, such as tetrahydrocortisol by means of 5 $\alpha$ -reductase, 5 $\beta$ -reductase and 3 $\alpha$ -hydroxysteroid dehydrogenase (Walker and Seckl, 2003). Repeating the assay with concomitant measurements of the aforementioned final metabolites and intermediates might shed further light on coronary artery endothelial steroid metabolism.

Earlier studies investigated the possibility of steroid synthesis outside the adrenal gland in cardiovascular tissues. mRNA for CYP11B1, 11 $\beta$ -hydroxylase, the rate-limiting enzyme for cortisol synthesis, was detected in cardiac tissue and aorta by northern blot (Kayes-Wandover and White, 2000) and inconsistently in failing human hearts by RT-PCR (Young *et al.*, 2001). Whether these transcripts were translated to proteins and, if so, their activity, were not assessed. The minuscule amount of cortisol detected in supernatants for DMSO-treated cells, although mostly above the limit of quantification, is negligible compared to the concentration of circulating steroids. Whether these concentrations might change in response to severe perturbations of homeostasis, such as in congestive heart failure, might be studied using ex vivo cultured hearts (Brandenburger *et al.*, 2012) to wash out systemic steroids. After the wash-out, tissue-specific synthesis might be assessed using MALDI imaging (Murakami *et al.*, 2019).

We consider it unlikely that the effects of 10 nM aldosterone on supernatant cortisone were due to stimulation with a falsely high aldosterone concentration: The aldosterone concentration in this group was very close to the intended 10 nM ( $10.350 \pm 0.431$  nM).

Antagonization of 100 nM aldosterone with eplerenone slightly but significantly reduced aldosterone supernatant concentrations. It may, thus, be that at high concentrations aldosterone inhibits its own metabolism via an MR-dependent mechanism. This could promote a feed-forward mechanism which further amplifies the potency of already elevated aldosterone concentrations. However, these concentrations are rarely observed in humans (Heinrich *et al.*, 2018) and it remains to be determined whether aldosterone metabolism in endothelial cells actually does occur *in vivo*. Aldosterone metabolites in general show drastically reduced bioactivity when compared to their mother substance. Morris and Brem compiled data which demonstrated that although aldosterone metabolites retain some antinatriuretic activity, the most bioactive metabolite, 5 $\alpha$ -dihydroaldosterone, possesses only 10 % of the original aldosterone activity (Morris and Brem, 1987).

As for cortisol metabolites, the experiments should be repeated with a broader lens i.e., an untargeted mass spectrometry approach to detect all hitherto described metabolites of aldosterone. From the respective product/educt ratios one could estimate activities of involved enzymes. This reverse approach may be more fruitful than determining mRNA levels which might not automatically equate protein activity.

#### 4.2.2 MR and GR marker gene transcription and interaction

In our experiments, we unfortunately could not establish FKBP5 as convincing transcriptional target of GR in human endothelial cells. Likewise, we could not confirm SCNN1A, the gene coding for ENaC channel alpha subunit, as a suitable marker of transcriptional activity for MR in this cell type. We could exclude that the rather low concentrations of aldosterone were the reason for these unexpected results because 10 and 100 nM aldosterone (both in addition to 140 nM cortisol) likewise did not result in significant expression changes.

No previous report using FKBP5 as transcriptional readout of GR stimulation in endothelial cells could be identified. Sekizawa and colleagues, using RNA-seq screen and validation via qPCR, described that treatment of endothelial cells with 1 nM aldosterone for 6 hours induces FKBP5 upregulation and is MR-dependent (Sekizawa *et al.*, 2011). In our approach this was not reproducible. One major difference to the experiments of Sekizawa *et al.* was that we had longer stimulation periods of 48 hours. The effect may be short lived and therefore not captured after 48 hours.

In human coronary artery smooth muscle cells, on the other hand, our group previously described an increase in FKBP5 transcription to cortisol stimulation by a factor of 20 (Brunnenkant *et al.*, 2021). It is conceivable that endothelial-specific regulatory mechanisms explain the comparatively small increase in FKBP5 upregulation in comparison to smooth muscle cells.

The ENaC channel, the alpha unit of which is coded for by the gene SCNN1A, is a well-established target of mineralocorticoid receptor stimulation. In epithelial tissues multiple mechanisms lead to increased MR-mediated ENaC conductance across cell membranes: MR directly fosters ENaC transcription, promotes insertion of pre-formed proteins into the membrane, prevents the internalization of membrane-standing ENaC proteins and their degradation, and increases ENaC open probability by SGK1-mediated phosphorylation (Zhang *et al.*, 2022). Studies using endothelial cells demonstrated that 10 nM aldosterone increase expression of  $\alpha$ -ENaC in HUVEC over a period of 72 hours by immunoblot. The same group also demonstrated increased surface abundance of  $\alpha$ -ENaC in HUVEC using quantum dot-coupled secondary antibodies for indirect immunofluorescence (Kusche-Vihrog *et al.*, 2008). Our findings are not in line with these results: We could not demonstrate an increase in SCNN1A transcript abundance in response to aldosterone, both in the absence or presence of concomitant cortisol stimulation.

It may be that an increase in SCNN1A transcription is transient and not measurable in states of chronic aldosterone excess. Alternatively, aldosterone may just have posttranslational effects, i.e. mediating membrane insertion of preformed ENaC molecules and/or stabilize ENaC by preventing premature protein degradation.

It is worth noting that the expression of SCNN1A in our cells was very low. The treatment condition which was associated with the highest expression levels (aldosterone+RU486) featured CT (cycle threshold) values of  $38.4 \pm 0.6$ . It is likely that the low expression levels negatively affected the sensitivity to detect minor expression changes which otherwise might have been uncovered. Further, there may be a disconnect in protein stability and mRNA turnover which could reconcile the low, aldosterone-unresponsive SCNN1A mRNA levels in our results and the aldosterone-dependent regulation demonstrated in other studies.

NFKBIA, the gene coding for nuclear factor  $\kappa$ B (NF $\kappa$ B) inhibitor  $\alpha$ , showed a significant increase in mRNA starting from a concentration of 10 nM aldosterone. NFKBIA had been confirmed to be a MR-responsive gene in human kidney cells and mRNA levels were found to be increased starting from 4 h after application of 10 nM aldosterone (Billan *et al.*, 2015).

Activation of NFKBIA transcription by glucocorticoids has been suggested to be part of a feedback control mechanism to curtail excessive NF $\kappa$ B-mediated inflammation (Newton *et al.*, 2017). Likewise, the induction of NFKBIA transcription in the experiments of this dissertation required co-stimulation with cortisol and was not apparent in cells solely treated with aldosterone, which renders its role as MR marker gene questionable.

In sum, a reliable, exclusive, endothelial transcriptional MR marker gene which also shows induction at lower concentrations such as 1 nM could not be identified in the present study.

Early studies on FKBP5 as a transcriptional marker for GR stimulation compared different glucocorticoids in their potency for FKBP5 induction. Hydrocortisone in a lymphoblast cell line led to prominent FKBP5 upregulation starting from concentrations of 1  $\mu$ M (Vermeer *et al.*, 2003). On the other hand, we could demonstrate in human coronary artery smooth muscle cells that 140 nM hydrocortisone induces a 20 fold increase in FKBP5 expression (Brunnenkant *et al.*, 2021). The reason why the same concentration in endothelial cells yielded no significant FKBP5

induction may be a cell-type specific regulation of GR transcriptional activity by additional co-regulators.

With the lack of robust and sensitive expression markers which showed a response at 1 nM aldosterone we could, thus, not reliably study the interaction of MR and GR signaling by qPCR in endothelial cells.

A possibility for future experiments might be the transfection of endothelial cells with MR and GR-specific luciferase reporter constructs like it has been described in COS-7 cells (Hellal-Levy *et al.*, 1999). Alternatively, truly endogenous MR- and GR-specific endothelial transcripts might be discovered using bulk RNA-sequencing of extracts from endothelial cells after stimulation with cortisol and aldosterone.

#### 4.2.3 Semiquantitative parallel analysis of MR and GR activation by immunofluorescence

Since we were not able to establish a reliable genetic readout for both MR and GR transcriptional activity, we changed our approach and focused on an imaging method. We tried to make use of the fact that transcriptionally active steroid receptors are typically found in the cellular nucleus while inactive receptors localize in the cytosol. While aldosterone at concentrations of 140 pM and 1 nM only showed a trend towards an increased MR signal in the nucleus, the same concentrations significantly decreased nuclear GR signals in a MR-dependent manner. As a caveat, cortisol did not increase the GR nuclear signal when compared to the DMSO control. It may, thus, be that either the cortisol concentration of 140 nM was too small or that a substantial proportion of GR molecules is activated at baseline.

Cytosolic GR exists as part of a multiprotein complex which involves, amongst others, hsp40, hsp56, hsp90 and src. In the ligand-free state the nuclear location sequence (NLS) of GR is not exposed. Upon ligand binding, GR dissociates from the complex, a process which uncovers the NLS and leads to the nuclear translocation (Revollo and Cidlowski, 2009),

Hartmann and co-workers described how baseline mineralocorticoid receptor expression levels regulates the neural stress response by glucocorticoid receptors in a manner involving MR-driven Fkbp5 expression and modulation of GR ligand affinity. Central to their findings is the notion that Fkbp5 expression is driven also by MR transactivation by glucocorticoids (Hartmann *et al.*, 2021). In our experiments nuclear translocation of GR was significantly inhibited by 1 nM aldosterone. Aldosterone at concentrations from 1 to 100 nM when administered simultaneously with 140 nM cortisol did not elicit a significant increase in FKBP5 transcript levels above those mediated by cortisol alone. Rather, a tendency of aldosterone to dose-dependently reduce FKBP5 expression was apparent, although this trend was not statistically significant. Taken together, increased MR-driven FKBP5 expression cannot explain the aldosterone-mediated inhibition of GR nuclear translocation. Interrogation of the remaining components of the cytosolic GR-multiprotein complex, including factors such as FKPB4 which is reported to increase GR ligand binding, might uncover how endothelial cells achieve antiparallel MR and GR nuclear translocation (Vandevyver, Dejager and Libert, 2012).

Data on competitive binding or functional antagonism of aldosterone at native glucocorticoid receptors are scarce and the literature provides evidence on single ligand binding to transfected receptors.

We present arguments for a functional antagonism of aldosterone at the glucocorticoid receptor. The level at which this antagonism took place may range all the way from competition for GR binding to post transcriptional mechanisms. Hellal-Levy and colleagues demonstrated that cortisol and aldosterone have comparable affinities for human GR (Hellal-Levy *et al.*, 1999). Cortisol in our experiments was used at 140-fold higher concentrations than aldosterone. Therefore, it is unlikely that displacement of cortisol from GR by aldosterone caused the 40 % reduction in nuclear GR localization. Using a reporter construct, the same publication by Hellal-Levy *et al.* showed that aldosterone at 1 nM was not able to induce any GR transcriptional activity while 100 nM cortisol yielded a full transcriptional effect.

Our study used a very late timepoint after stimulation with GR and MR agonists (48 hours). Typical timepoints for studying nuclear translocation of these receptors are 1-2 hours (Boix *et al.*, 2017). It may be that the subcellular localization of GR and MR changes after prolonged stimulation. In line with this reasoning, GR were reported to shuttle across nuclear membranes in a bidirectional manner (Madan and Defranco, 1993). This mechanism may have blurred the impact of aldosterone on GR localization. Limiting the steroid exposure to shorter timeframes might yield clearer results, possibly also for the MR localization experiments.

In sum, we cannot assume a prominent role of aldosterone signaling in endothelial cells. This is reflected by low baseline expression of MR-selective marker genes and the inability to demonstrate an aldosterone-dependent gene induction in the presence of competing cortisol concentrations.

Our final conclusion from chapter B is that mineralocorticoid receptors in endothelial cells are unprotected from circulating cortisol. We found signals that aldosterone functionally antagonizes glucocorticoid receptor nuclear translocation, although we could not corroborate these findings at the transcript level.

## References

Archer, S. L. et al. (2003) 'Endothelium-Derived Hyperpolarizing Factor in Human Internal Mammary Artery Is 11,12-Epoxyeicosatrienoic Acid and Causes Relaxation by Activating Smooth Muscle BKCa Channels', *Circulation*, 107(5), pp. 769–776. doi: 10.1161/01.CIR.0000047278.28407.C2.

Arlt, W. et al. (2017) 'Steroid metabolome analysis reveals prevalent glucocorticoid excess in primary aldosteronism', *JCI insight*, 2(8), pp. 0–14. doi: 10.1172/jci.insight.93136.

Bagher, P. et al. (2012) 'Low intravascular pressure activates endothelial cell TRPV4 channels, local Ca<sup>2+</sup> events, and IKCa channels, reducing arteriolar tone.', *Proceedings of the National Academy of Sciences of the United States of America*, 109(44), pp. 18174–9. doi: 10.1073/pnas.1211946109.

Bernini, G. et al. (2008) 'Arterial stiffness, intima-media thickness and carotid artery fibrosis in patients with primary aldosteronism.', *Journal of hypertension*, 26(12), pp. 2399–2405. doi: 10.1097/HJH.0b013e32831286fd.

Billan, F. Le et al. (2015) 'Cistrome of the aldosterone-activated mineralocorticoid receptor in human renal cells', *FASEB Journal*, 29(9), pp. 3977–3989. doi: 10.1096/fj.15-274266.

Boix, J. et al. (2017) 'Primary aldosteronism patients show skin alterations and abnormal activation of glucocorticoid receptor in keratinocytes', *Scientific Reports*, 7(1), pp. 1–10. doi: 10.1038/s41598-017-16216-5.

Brandenburger, M. et al. (2012) 'Organotypic slice culture from human adult ventricular myocardium', *Cardiovascular Research*, 93(1), pp. 50–59. doi: 10.1093/cvr/cvr259.

Braun, L. T., Vogel, F. and Reincke, M. (2022) 'Long-term morbidity and mortality in patients with Cushing's syndrome', *Journal of Neuroendocrinology*, (February), pp. 1–11. doi: 10.1111/jne.13113.

Brem, A. S. et al. (1998) 'Localization of 2 11 $\beta$ -OH Steroid Dehydrogenase Isoforms in Aortic Endothelial Cells', *Hypertension*, 31(1), pp. 459–462. doi: 10.1161/01.HYP.31.1.459.

Brunnenkant, L. et al. (2021) *Supplement - Intact EET pathway in hyperaldosteronism*, *BioRxiv*. Available at: <https://www.biorxiv.org/content/10.1101/2021.02.04.429624v1.supplementary-material> (Accessed: 3 February 2021).

Busse, R. et al. (1988) 'Hyperpolarization and increased free calcium in acetylcholine-stimulated endothelial cells', *American Journal of Physiology - Heart and Circulatory Physiology*, 255(4). doi: 10.1152/ajpheart.1988.255.4.h965.

Campbell, W. B. et al. (1996) 'Identification of Epoxyeicosatrienoic Acids as Endothelium-Derived Hyperpolarizing Factors', *Circulation Research*, 78(3), pp. 415–423. doi: 10.1161/01.RES.78.3.415.

Caulfield, M. P. and Birdsall, N. J. M. (1998) 'International union of pharmacology. XVII. Classification of muscarinic acetylcholine receptors', *Pharmacological Reviews*, 50(2), pp. 279–290.

Van Cauter, E., Leproult, R. and Kupfer, D. J. (1996) 'Effects of gender and age on the levels and circadian rhythmicity of plasma cortisol', *Journal of Clinical Endocrinology and Metabolism*, 81(7), pp. 2468–2473. doi: 10.1210/jc.81.7.2468.

Chan, C.-K. et al. (2020) 'Arterial Stiffness Is Associated with Clinical Outcome and Cardiorenal Injury in Lateralized Primary Aldosteronism', *The Journal of Clinical Endocrinology & Metabolism*, 105(11), pp. e3950–e3960. doi: 10.1210/clinem/dgaa566.

Chan, S. Y. et al. (2003) 'The prognostic importance of endothelial dysfunction and carotid atheroma burden in patients with coronary artery disease', *Journal of the American College of Cardiology*. Elsevier Masson SAS, 42(6), pp. 1037–1043. doi: 10.1016/S0735-1097(03)00927-6.

Chapman, K., Holmes, M. and Seckl, J. (2013) '11 $\beta$ -Hydroxysteroid Dehydrogenases:

Intracellular Gate-Keepers of Tissue Glucocorticoid Action', *Physiological Reviews*, 93(3), pp. 1139–1206. doi: 10.1152/physrev.00020.2012.

Christy, C. et al. (2003) '11 $\beta$ -hydroxysteroid dehydrogenase type 2 in mouse aorta: Localization and influence on response to glucocorticoids', *Hypertension*, 42(4 I), pp. 580–587. doi: 10.1161/01.HYP.0000088855.06598.5B.

DeLozier, T. C. et al. (2007) 'Detection of human CYP2C8, CYP2C9, and CYP2J2 in cardiovascular tissues', *Drug Metabolism and Disposition*, 35(4), pp. 682–688. doi: 10.1124/dmd.106.012823.

Deng, Y. et al. (2011) 'Endothelial CYP epoxygenase overexpression and soluble epoxide hydrolase disruption attenuate acute vascular inflammatory responses in mice', *The FASEB Journal*, 25(2), pp. 703–713. doi: 10.1096/fj.10-171488.

Dinh, Q. N. et al. (2020) 'Aldosterone-Induced Hypertension is Sex-Dependent, Mediated by T Cells and Sensitive to GPER Activation', *Cardiovascular Research*, 53(9), pp. 1689–1699. doi: 10.1093/cvr/cvaa075.

Draper, A. J. and Hammock, B. D. (1999) 'Inhibition of soluble and microsomal epoxide hydrolase by zinc and other metals', *Toxicological Sciences*, 52(1), pp. 26–32. doi: 10.1093/toxsci/52.1.26.

Edin, M. L. et al. (2018) 'Epoxide hydrolase 1 (EPHX1) hydrolyzes epoxyeicosanoids and impairs cardiac recovery after ischemia', *Journal of Biological Chemistry*, 293(9), pp. 3281–3292. doi: 10.1074/jbc.RA117.000298.

Edwards, C. R. W. et al. (1988) 'Localisation of 11 beta-hydroxysteroid dehydrogenase--tissue specific protector of the mineralocorticoid receptor', *The Lancet*, 332(8618), pp. 986–989. doi: 10.1016/S0140-6736(88)90742-8.

Edwards, G. et al. (1998) 'K<sup>+</sup> is an endothelium-derived hyperpolarizing factor in rat arteries.', *Nature*. doi: 10.1038/24388.

Falcone, J. C. (1995) 'Endothelial cell calcium and vascular control.', *Medicine and science in sports and exercise*, 27(8), pp. 1165–9. Available at: <http://www.ncbi.nlm.nih.gov/pubmed/7476061>.

Falcone, J. C., Kuo, L. and Meininger, G. A. (1993) 'Endothelial cell calcium increases during flow-induced dilation in isolated arterioles', *American Journal of Physiology - Heart and Circulatory Physiology*, 264(2 33-2). doi: 10.1152/ajpheart.1993.264.2.h653.

Fang, X., Weintraub, N. L. and Spector, A. A. (2003) 'Differences in positional esterification of 14,15-epoxyeicosatrienoic acid in phosphatidylcholine of porcine coronary artery endothelial and smooth muscle cells', *Prostaglandins and Other Lipid Mediators*, 71(1–2), pp. 33–42. doi: 10.1016/S0090-6980(03)00002-9.

Farin, F. M., Pohlman, T. H. and Omiecinski, C. J. (1994) 'Expression of Cytochrome P450s and Microsomal Epoxide Hydrolase in Primary Cultures of Human Umbilical Vein Endothelial Cells', *Toxicology and Applied Pharmacology*, 124(1), pp. 1–9. doi: 10.1006/taap.1994.1001.

Favre, J. et al. (2011) 'Coronary endothelial dysfunction after cardiomyocyte-specific mineralocorticoid receptor overexpression', *American Journal of Physiology - Heart and Circulatory Physiology*, 300(6), pp. 2035–2043. doi: 10.1152/ajpheart.00552.2010.

Féletalou, M. and Vanhoutte, P. M. (2009) 'EDHF: An update', *Clinical science (London, England : 1979)*, 117(4), pp. 139–55. doi: 10.1042/CS20090096.

Fisslthaler, B. et al. (1999) 'Cytochrome P450 2C is an EDHF synthase in coronary arteries.', *Nature*, 401(6752), pp. 493–7. doi: 10.1038/46816.

Fisslthaler, B. et al. (2001) 'Cyclic stretch enhances the expression and activity of coronary endothelium-derived hyperpolarizing factor synthase', *Hypertension*, 38(6), pp. 1427–1432. doi: 10.1161/hy1201.096532.

Freel, E. M. et al. (2012) 'Demonstration of blood pressure-independent noninfarct myocardial fibrosis in primary aldosteronism: A cardiac magnetic resonance imaging study', *Circulation: Cardiovascular Imaging*, 5(6), pp. 740–747. doi: 10.1161/CIRCIMAGING.112.974576.

Fukushima, K. et al. (2005) 'Aldosterone enhances 11 $\beta$ -hydroxysteroid dehydrogenase type 2

expression in colonic epithelial cells *in vivo*', *Scandinavian Journal of Gastroenterology*, 40(7), pp. 850–857. doi: 10.1080/00365520510015700.

Funder, J. W. *et al.* (1988) 'Mineralocorticoid Action: Target Tissue Specificity Is Enzyme, Not Receptor, Mediated', *Science*, 242(4878), pp. 583–585. doi: 10.1126/science.2845584.

Funder, J. W. *et al.* (2016) 'The Management of Primary Aldosteronism: Case Detection, Diagnosis, and Treatment: An Endocrine Society Clinical Practice Guideline', *The Journal of Clinical Endocrinology & Metabolism*, 101(5), pp. 1889–1916. doi: 10.1210/jc.2015-4061.

Funder, J. W. and Carey, R. M. (2022) 'Primary Aldosteronism: Where Are We Now? Where to From Here?', *Hypertension*, (April), pp. 1–10. doi: 10.1161/hypertensionaha.121.18761.

Furchtgott, R. F. and Zawadzki, J. V. (1980) 'The obligatory role of endothelial cells in the relaxation of arterial smooth muscle by acetylcholine', *Nature*, 288(5789), pp. 373–376. doi: 10.1038/288373a0.

Gauthier, K. M. *et al.* (2002) '14,15-Epoxyeicosa-5( Z )-enoic Acid A Selective Epoxyeicosatrienoic Acid Antagonist That Inhibits Endothelium-Dependent Hyperpolarization and Relaxation in Coronary Arteries', *Circulation Research*, 90(9), pp. 1028–1036. doi: 10.1161/01.res.0000018162.87285.f8.

Gauthier, K. M. *et al.* (2005) '14,15-Epoxyeicosatrienoic acid represents a transferable endothelium-dependent relaxing factor in bovine coronary arteries', *Hypertension*, 45(4 SUPPL.), pp. 666–671. doi: 10.1161/01.HYP.0000153462.06604.5d.

Gimbrone, M. A. and García-Cardeña, G. (2016) 'Endothelial Cell Dysfunction and the Pathobiology of Atherosclerosis', *Circulation Research*, 118(4), pp. 620–636. doi: 10.1161/CIRCRESAHA.115.306301.

Gong, R., Morris, D. J. and Brem, A. S. (2008) 'Variable expression of 11 $\beta$  Hydroxysteroid dehydrogenase (11 $\beta$ -HSD) isoforms in vascular endothelial cells', *Steroids*, 73(11), pp. 1187–1196. doi: 10.1016/j.steroids.2008.05.009.

Gros, R. *et al.* (2011) 'GPR30 expression is required for the mineralocorticoid receptor-independent rapid vascular effects of aldosterone', *Hypertension*, 57(3), pp. 442–451. doi: 10.1161/HYPERTENSIONAHA.110.161653.

Gupta, N. C. *et al.* (2012) 'Soluble epoxide hydrolase: Sex differences and role in endothelial cell survival', *Arteriosclerosis, Thrombosis, and Vascular Biology*, 32(8), pp. 1936–1942. doi: 10.1161/ATVBAHA.112.251520.

Hadoke, P. W. F. *et al.* (2001) 'Endothelial Cell Dysfunction in Mice After Transgenic Knockout of Type 2, but Not Type 1, 11 $\beta$ -Hydroxysteroid Dehydrogenase', *Circulation*, 104(23), pp. 2832–2837. doi: 10.1161/hc4801.100077.

Halcox, J. P. J. *et al.* (2009) 'Endothelial function predicts progression of carotid intima-media thickness', *Circulation*, 119(7), pp. 1005–1012. doi: 10.1161/CIRCULATIONAHA.108.765701.

Hannemann, A. *et al.* (2011) 'Plasma aldosterone levels and aldosterone-to-renin ratios are associated with endothelial dysfunction in young to middle-aged subjects', *Atherosclerosis*. Elsevier Ireland Ltd, 219(2), pp. 875–879. doi: 10.1016/j.atherosclerosis.2011.09.008.

Hartmann, J. *et al.* (2021) 'Mineralocorticoid receptors dampen glucocorticoid receptor sensitivity to stress via regulation of FKBP5', *Cell Reports*, 35(9). doi: 10.1016/j.celrep.2021.109185.

Heinrich, D. A. *et al.* (2018) 'Primary aldosteronism : key characteristics at diagnosis : a trend toward milder forms', *European Journal of Endocrinology*, 178(6), pp. 605–611.

Hellal-Levy, C. *et al.* (1999) 'Specific hydroxylations determine selective corticosteroid recognition by human glucocorticoid and mineralocorticoid receptors', *FEBS Letters*, 464(1–2), pp. 9–13. doi: 10.1016/S0014-5793(99)01667-1.

Huang, T. *et al.* (2000) 'Heterogeneity of [Ca 2+]i signaling in intact rat aortic endothelium', *The FASEB Journal*, 14(5), pp. 797–804. doi: 10.1096/fasebj.14.5.797.

Hudson, W. H., Youn, C. and Ortlund, E. A. (2014) 'Crystal structure of the mineralocorticoid receptor DNA binding domain in complex with DNA', *PLoS ONE*, 9(9), pp. 1–9. doi: 10.1371/journal.pone.0107000.

Hundemer, G. et al. (2018) 'Cardiometabolic outcomes and mortality in medically treated primary aldosteronism: a retrospective cohort study.', *The Lancet Diabetes and Endocrinology*, 6(1), pp. 51–59.

Hundemer, G. L. et al. (2018a) 'Incidence of atrial fibrillation and mineralocorticoid receptor activity in patients with medically and surgically treated primary aldosteronism', *JAMA Cardiology*, 3(8), pp. 768–774. doi: 10.1001/jamacardio.2018.2003.

Hundemer, G. L. et al. (2018b) 'Renal outcomes in medically and surgically treated primary aldosteronism', *Hypertension*, 72(3), pp. 658–666. doi: 10.1161/HYPERTENSIONAHA.118.11568.

Hung, C.-S. et al. (2019) 'Aldosterone induces vascular damage - a wave reflection analysis study', *Hypertension*, (7), pp. 1–7. doi: 10.1161/HYPERTENSIONAHA.118.12342.

Imig, J. D. (2012) 'Epoxides and Soluble Epoxide Hydrolase in Cardiovascular Physiology', *Physiological Reviews*, 92(1), pp. 101–130. doi: 10.1152/physrev.00021.2011.

Imig, J. D., Jankiewicz, W. K. and Khan, A. H. (2020) 'Epoxy Fatty Acids: From Salt Regulation to Kidney and Cardiovascular Therapeutics', *Hypertension*, pp. 3–15. doi: 10.1161/hypertensionaha.120.13898.

Jiang, H., Anderson, G. D. and McGiff, J. C. (2010) 'Red blood cells (RBCs), epoxyeicosatrienoic acids (EETs) and adenosine triphosphate (ATP)', *Pharmacological Reports*, 62(3), pp. 468–474. doi: 10.1016/S1734-1140(10)70302-9.

Kayes-Wandover, K. M. and White, P. C. (2000) 'Steroidogenic Enzyme Gene Expression in the Human Heart', *The Journal of Clinical Endocrinology & Metabolism*, 85(7), pp. 2519–2525. doi: 10.1210/jcem.85.7.6663.

Kishimoto, S. et al. (2018) 'Eplerenone improves endothelial function and arterial stiffness and inhibits Rho-associated kinase activity in patients with idiopathic hyperaldosteronism', *Journal of Hypertension*, p. 1. doi: 10.1097/HJH.0000000000001989.

Kishimoto, S. et al. (2020) 'A Comparison of Adrenalectomy and Eplerenone on Vascular Function in Patients with Aldosterone-producing Adenoma', *The Journal of Clinical Endocrinology & Metabolism*, 105(11), pp. 2341–2386. doi: 10.1210/clinem/dgaa561.

Köhler, R. et al. (2001) 'Expression of ryanodine receptor type 3 and TRP channels in endothelial cells: Comparison of in situ and cultured human endothelial cells', *Cardiovascular Research*, 51(1), pp. 160–168. doi: 10.1016/S0008-6363(01)00281-4.

Kovacic, J. C. et al. (2019) 'Endothelial to Mesenchymal Transition in Cardiovascular Disease: JACC State-of-the-Art Review', *Journal of the American College of Cardiology*, 73(2), pp. 190–209. doi: 10.1016/j.jacc.2018.09.089.

Kusche-Vihrog, K. et al. (2008) 'Aldosterone and amiloride alter ENaC abundance in vascular endothelium', *Pflugers Archiv European Journal of Physiology*, 455(5), pp. 849–857. doi: 10.1007/s00424-007-0341-0.

Larsen, B. T. et al. (2006) 'Epoxyeicosatrienoic and dihydroxyeicosatrienoic acids dilate human coronary arterioles via BKCa channels: Implications for soluble epoxide hydrolase inhibition', *American Journal of Physiology - Heart and Circulatory Physiology*, 290(2), pp. 491–499. doi: 10.1152/ajpheart.00927.2005.

Ledoux, J. et al. (2008) 'Functional architecture of inositol 1,4,5-trisphosphate signaling in restricted spaces of myoendothelial projections', *Proceedings of the National Academy of Sciences of the United States of America*, 105(28), pp. 9627–9632. doi: 10.1073/pnas.0801963105.

Lee, D. L. et al. (2011) 'Peroxisome proliferator-activated receptor- $\alpha$  activation decreases mean arterial pressure, plasma interleukin-6, and COX-2 while increasing renal CYP4A expression in an acute model of DOCA-salt hypertension', *PPAR Research*, 2011. doi: 10.1155/2011/502631.

Leopold, J. A. et al. (2007) 'Aldosterone impairs vascular reactivity by decreasing glucose-6-phosphate dehydrogenase activity', *Nature Medicine*, 13(2), pp. 189–197. doi: 10.1038/nm1545.

Liang, S. H., Hassett, C. and Omiecinski, C. J. (2005) 'Alternative promoters determine tissue-specific expression profiles of the human microsomal epoxide hydrolase gene (EPHX1)', *Molecular Pharmacology*, 67(1), pp. 220–230. doi: 10.1124/mol.104.005579.

Lin, Y. H. *et al.* (2012) 'Adrenalectomy improves increased carotid intima-media thickness and arterial stiffness in patients with aldosterone producing adenoma', *Atherosclerosis*. Elsevier Ireland Ltd, 221(1), pp. 154–159. doi: 10.1016/j.atherosclerosis.2011.12.003.

Liu, P. *et al.* (2018) 'Downregulated Serum 14, 15-Epoxyeicosatrienoic Acid Is Associated With Abdominal Aortic Calcification in Patients With Primary Aldosteronism', *Hypertension*, 71(4), pp. 592–598. doi: 10.1161/HYPERTENSIONAHA.117.10644.

Liu, Y. *et al.* (2009) 'Glucocorticoid response elements and 11 $\beta$ -hydroxysteroid dehydrogenases in the regulation of endothelial nitric oxide synthase expression', *Cardiovascular Research*, 81(1), pp. 140–147. doi: 10.1093/cvr/cvn231.

Loch, D. *et al.* (2007) 'Prevention of hypertension in DOCA-salt rats by an inhibitor of soluble epoxide hydrolase', *Cell Biochem Biophys*, 47(1), pp. 87–98. doi: CBB:47:1:87 [pii].

Lubitz, C. C. *et al.* (2015) 'Cost-Effectiveness of Screening for Primary Aldosteronism and Subtype Diagnosis in the Resistant Hypertensive Patients', *Circulation: Cardiovascular Quality and Outcomes*, 8(6), pp. 621–630. doi: 10.1161/CIRCOUTCOMES.115.002002.

Luo, J., Busillo, J. M. and Benovic, J. L. (2008) 'M 3 Muscarinic Acetylcholine Receptor-Mediated Signaling Is Regulated by Distinct Mechanisms', *Molecular Pharmacology*, 74(2), pp. 338–347. doi: 10.1124/mol.107.044750.

Luther, J. M. *et al.* (2021) 'Treatment of Primary Aldosteronism Increases Plasma Epoxyeicosatrienoic Acids', *Hypertension*, (April), pp. 1–9. doi: 10.1161/HYPERTENSIONAHA.120.14808.

Madan, A. P. and Defranco, D. B. (1993) 'Bidirectional transport of glucocorticoid receptors across the nuclear envelope', *Proceedings of the National Academy of Sciences of the United States of America*, 90(8), pp. 3588–3592. doi: 10.1073/pnas.90.8.3588.

Marowsky, A. *et al.* (2009) 'Distribution of soluble and microsomal epoxide hydrolase in the mouse brain and its contribution to cerebral epoxyeicosatrienoic acid metabolism', *Neuroscience*. Elsevier Inc., 163(2), pp. 646–661. doi: 10.1016/j.neuroscience.2009.06.033.

Matoba, T. *et al.* (2000) 'Hydrogen peroxide is an endothelium-derived hyperpolarizing factor in mice.', *The Journal of clinical investigation*, 106(12), pp. 1521–1530. doi: 10.1172/JCI10506.

Matsumoto, T. *et al.* (2015) 'Effect of Aldosterone-Producing Adenoma on Endothelial Function and Rho-Associated Kinase Activity in Patients With Primary Aldosteronism', *Hypertension*, 65(3), pp. 841–848. doi: 10.1161/HYPERTENSIONAHA.114.

Mihailidou, A. S. *et al.* (2009) 'Glucocorticoids activate cardiac mineralocorticoid receptors during experimental myocardial infarction', *Hypertension*, 54(6), pp. 1306–1312. doi: 10.1161/HYPERTENSIONAHA.109.136242.

Milliez, P. *et al.* (2005) 'Evidence for an increased rate of cardiovascular events in patients with primary aldosteronism', *Journal of the American College of Cardiology*, 45(8), pp. 1243–1248. doi: 10.1016/j.jacc.2005.01.015.

Moncada, S. and Vane, J. R. (1978) 'Pharmacology and endogenous roles of prostaglandin endoperoxides, thromboxane A2, and prostacyclin', *Pharmacological Reviews*, 30(3), pp. 293–331.

Monticone, S. *et al.* (2017) 'Prevalence and Clinical Manifestations of Primary Aldosteronism Encountered in Primary Care Practice', *Journal of the American College of Cardiology*, 69(14), pp. 1811–1820. doi: 10.1016/j.jacc.2017.01.052.

Morris, D. J. and Brem, A. S. (1987) 'Metabolic derivatives of aldosterone', *American Journal of Physiology - Renal Fluid and Electrolyte Physiology*, 252(3 (21/3)). doi: 10.1152/ajprenal.1987.252.3.f365.

Moser, M. *et al.* (2018) 'Endothelial cell mineralocorticoid receptors oppose VEGF-induced gene expression and angiogenesis', *Journal of Endocrinology*, 240(1), pp. 15–26. doi: 10.1530/joe-18-0494.

Mulvany, M. J. and Aalkjaer, C. (1990) 'Structure and Function of Small Arteries', *Physiological reviews*, 70(4), pp. 921–961.

Murakami, M. *et al.* (2019) 'In situ metabolomics of aldosterone-producing adenomas', *JCI*

*Insight*, 4(17), pp. 1–15. doi: 10.1172/jci.insight.130356.

Nagata, D. et al. (2006) 'Molecular mechanism of the inhibitory effect of aldosterone on endothelial NO synthase activity', *Hypertension*, 48(1), pp. 165–171. doi: 10.1161/01.HYP.0000226054.53527.bb.

Newton, R. et al. (2017) 'Glucocorticoid and cytokine crosstalk: Feedback, feedforward, and co-regulatory interactions determine repression or resistance', *Journal of Biological Chemistry*. © 2017 ASBMB. Currently published by Elsevier Inc; originally published by American Society for Biochemistry and Molecular Biology., 292(17), pp. 7163–7172. doi: 10.1074/jbc.R117.777318.

Nishizaka, M. K. et al. (2004) 'Impaired endothelium-dependent flow-mediated vasodilation in hypertensive subjects with hyperaldosteronism', *Circulation*, 109(23), pp. 2857–2861. doi: 10.1161/01.CIR.0000129307.26791.8E.

Nithipatikom, K., Pratt, P. and Campbell, W. B. (2000) 'Determination of EETs using microbore liquid chromatography with fluorescence detection', *American Journal of Physiology - Heart and Circulatory Physiology*, 279(2), pp. H857–H862.

Oberleithner, H. et al. (2009) 'Potassium softens vascular endothelium and increases nitric oxide release.', *Proceedings of the National Academy of Sciences of the United States of America*, 106, pp. 2829–2834. doi: 10.1073/pnas.0813069106.

Ohno, Y. et al. (2018) 'Prevalence of Cardiovascular Disease and Its Risk Factors in Primary Aldosteronism: A Multicenter Study in Japan.', *Hypertension*, 71(3), pp. 530–537. doi: 10.1161/HYPERTENSIONAHA.117.10263.

Okada, T. et al. (2017) 'N-3 polyunsaturated fatty acids decrease the protein expression of soluble epoxide hydrolase via oxidative stress-induced P38 kinase in rat endothelial cells', *Nutrients*, 9(7), pp. 1–14. doi: 10.3390/nu9070654.

Oni-Orisan, A. et al. (2016) 'Cytochrome P450-derived epoxyeicosatrienoic acids and coronary artery disease in humans: a targeted metabolomics study', *Journal of Lipid Research*, 57(1), pp. 109–119. doi: 10.1194/jlr.M061697.

Ottolini, M., Hong, K. and Sonkusare, S. K. (2019) 'Calcium signals that determine vascular resistance', *Wiley Interdisciplinary Reviews: Systems Biology and Medicine*, 11(5), pp. 1–27. doi: 10.1002/wsbm.1448.

Rand, V. E. and Garland, C. J. (1992) 'Endothelium-dependent relaxation to acetylcholine in the rabbit basilar artery: importance of membrane hyperpolarization', *British Journal of Pharmacology*, 106(1), pp. 143–150. doi: 10.1111/j.1476-5381.1992.tb14307.x.

Reincke, M. et al. (2012) 'Observational study mortality in treated primary aldosteronism: The German conn's registry', *Hypertension*, 60(3), pp. 618–624. doi: 10.1161/HYPERTENSIONAHA.112.197111.

Reincke, M. (2018) 'Primary Aldosteronism and Cardiovascular Events - It Is Time to Take Guideline Recommendations Seriously', *Hypertension*, 71(3), pp. 413–414. doi: 10.3014/updates.2092.

Reincke, M. et al. (2021) 'Diagnosis and treatment of primary aldosteronism', *The Lancet Diabetes & Endocrinology*, 9(12), pp. 876–892. doi: 10.1016/S2213-8587(21)00210-2.

Revollo, J. R. and Cidlowski, J. A. (2009) 'Mechanisms generating diversity in glucocorticoid receptor signaling', *Annals of the New York Academy of Sciences*, 1179, pp. 167–178. doi: 10.1111/j.1749-6632.2009.04986.x.

Rogers, K. M. et al. (2002) 'Inhibitory effect of glucocorticoid on coronary artery endothelial function', *American Journal of Physiology - Heart and Circulatory Physiology*, 283(5 52-5), pp. 1922–1928. doi: 10.1152/ajpheart.00364.2002.

Rosolowsky, M. and Campbell, W. B. (1993) 'Role of PGI2 and epoxyeicosatrienoic acids in relaxation of bovine coronary arteries to arachidonic acid', *American Journal of Physiology - Heart and Circulatory Physiology*, 264(2 33-2). doi: 10.1152/ajpheart.1993.264.2.h327.

Rupprecht, R. et al. (1993) 'Pharmacological and functional characterization of human mineralocorticoid and glucocorticoid receptor ligands', *European Journal of Pharmacology: Molecular Pharmacology*, 247(2), pp. 145–154. doi: 10.1016/0922-4106(93)90072-H.

Savard, S. et al. (2013) 'Cardiovascular Complications Associated With Primary Aldosteronism: A Controlled Cross-Sectional Study', *Hypertension*, 62(2), pp. 331–336. doi: 10.1161/HYPERTENSIONAHA.113.01060.

Schindelin, J. et al. (2012) 'Fiji: An open-source platform for biological-image analysis', *Nature Methods*, 9(7), pp. 676–682. doi: 10.1038/nmeth.2019.

Sekizawa, N. et al. (2011) 'Transcriptome analysis of aldosterone-regulated genes in human vascular endothelial cell lines stably expressing mineralocorticoid receptor', *Molecular and Cellular Endocrinology*. Elsevier Ireland Ltd, 341(1–2), pp. 78–88. doi: 10.1016/j.mce.2011.05.029.

Sinal, C. J. et al. (2000) 'Targeted disruption of soluble epoxide hydrolase reveals a role in blood pressure regulation', *Journal of Biological Chemistry*, 275(51), pp. 40504–40510. doi: 10.1074/jbc.M008106200.

Sonkusare, S. K. et al. (2012) 'Elementary Ca<sup>2+</sup> signals through endothelial TRPV4 channels regulate vascular function.', *Science (New York, N.Y.)*, 336(6081), pp. 597–601. doi: 10.1126/science.1216283.

Spector, A. A. et al. (2004) 'Epoxyeicosatrienoic acids (EETs): Metabolism and biochemical function', *Progress in Lipid Research*, 43(1), pp. 55–90. doi: 10.1016/S0163-7827(03)00049-3.

Stewart, P. M. et al. (1987) 'Mineralocorticoid Activity of Liquorice: 11-Beta-Hydroxysteroid Dehydrogenase Deficiency Comes of Age', *The Lancet*, 330(8563), pp. 821–824. doi: 10.1016/S0140-6736(87)91014-2.

Stewart, P. M. et al. (1988) 'Syndrome of apparent mineralocorticoid excess. A defect in the cortisol-cortisone shuttle', *Journal of Clinical Investigation*, 82(1), pp. 340–349. doi: 10.1172/JCI113592.

Štrauch, B. et al. (2006) 'Increased Arterial Wall Stiffness in Primary Aldosteronism in Comparison With Essential Hypertension', *American Journal of Hypertension*, 19(9), pp. 909–914. doi: 10.1016/j.amjhyper.2006.02.002.

Taddei, S. et al. (2000) 'Physical activity prevents age-related impairment in nitric oxide availability in elderly athletes', *Circulation*, 101(25), pp. 2896–2901. doi: 10.1161/01.CIR.101.25.2896.

Takeda, M. et al. (2018) 'Clinical characteristics and postoperative outcomes of primary aldosteronism in the elderly', *Journal of Clinical Endocrinology and Metabolism*, 103(10), pp. 3620–3629. doi: 10.1210/jc.2018-00059.

Thies, R. L. and Autor, A. P. (1991) 'Reactive oxygen injury to cultured pulmonary artery endothelial cells: Mediation by poly(ADP-ribose) polymerase activation causing NAD depletion and altered energy balance', *Archives of Biochemistry and Biophysics*, 286(2), pp. 353–363. doi: 10.1016/0003-9861(91)90051-J.

Tsuchiya, K., Yoshimoto, T. and Hirata, Y. (2009) 'Endothelial dysfunction is related to aldosterone excess and raised blood pressure.', *Endocrine journal*, 56(4), pp. 553–9. doi: 10.1507/endocrj.K09E-014.

Vandevyver, S., Dejager, L. and Libert, C. (2012) 'On the Trail of the Glucocorticoid Receptor: Into the Nucleus and Back', *Traffic*, 13(3), pp. 364–374. doi: 10.1111/j.1600-0854.2011.01288.x.

Vermeer, H. et al. (2003) 'Glucocorticoid-induced increase in lymphocytic FKBP51 messenger ribonucleic acid expression: A potential marker for glucocorticoid sensitivity, potency, and bioavailability', *Journal of Clinical Endocrinology and Metabolism*, 88(1), pp. 277–284. doi: 10.1210/jc.2002-020354.

Vögler, O. et al. (1999) 'Regulation of muscarinic acetylcholine receptor sequestration and function by β-arrestin', *Journal of Biological Chemistry*, 274(18), pp. 12333–12338. doi: 10.1074/jbc.274.18.12333.

Vriens, J. et al. (2005) 'Modulation of the Ca<sup>2+</sup> permeable cation channel TRPV4 by cytochrome P450 epoxygenases in vascular endothelium', *Circulation Research*, 97(9), pp. 908–915. doi: 10.1161/01.RES.0000187474.47805.30.

Walker, B. R. and Seckl, J. R. (2003) 'Cortisol Metabolism', *International Textbook of Obesity*, 988707, pp. 241–268. doi: 10.1002/0470846739.ch18.

Watanabe, D. *et al.* (2021) 'Clinical impacts of endothelium-dependent flow-mediated vasodilation assessment on primary aldosteronism', *Endocrine Connections*, 10(6), pp. 578–587. doi: 10.1530/EC-21-0057.

Watanabe, H. *et al.* (2003) 'Anandamide and arachidonic acid use epoxyeicosatrienoic acids to activate TRPV4 channels', *Nature*, 424(6947), pp. 434–438. doi: 10.1038/nature01807.

Williams, T. A. *et al.* (2017) 'Outcomes after adrenalectomy for unilateral primary aldosteronism: An international consensus on outcome measures and analysis of remission rates in an international cohort', *The Lancet Diabetes and Endocrinology*, 5(9), pp. 689–699. doi: 10.1016/S2213-8587(17)30135-3.

Wu, S. *et al.* (1996) 'Molecular Cloning and Expression of CYP2J2, a Human Cytochrome P450 Arachidonic Acid Epoxygenase Highly Expressed in Heart', *Journal of Biological Chemistry*, 271(7), pp. 3460–3468. doi: 10.1074/jbc.271.7.3460.

Xu, Z. *et al.* (2020) 'Primary Aldosteronism in Patients in China With Recently Detected Hypertension', *Journal of the American College of Cardiology*, 75(16), pp. 1913–1922. doi: 10.1016/j.jacc.2020.02.052.

Young, M. J. *et al.* (2001) 'Cardiac steroidogenesis in the normal and failing heart', *Journal of Clinical Endocrinology and Metabolism*, 86(11), pp. 5121–5126. doi: 10.1210/jcem.86.11.7925.

Yu, Z. *et al.* (2004) 'Vascular localization of soluble epoxide hydrolase in the human kidney', *American Journal of Physiology - Renal Physiology*, 286(4 55-4), pp. 720–726. doi: 10.1152/ajprenal.00165.2003.

Yuan, Y. *et al.* (2021) 'Plasma aldosterone concentration is associated with white matter lesions in patients with primary aldosteronism', *Endocrine*. Springer US. doi: 10.1007/s12020-021-02920-w.

Zeldin, D. C. *et al.* (1995) 'Molecular cloning, expression and characterization of an endogenous human cytochrome P450 arachidonic acid epoxygenase isoform', *Archives of Biochemistry and Biophysics*, pp. 76–86. doi: 10.1006/abbi.1995.1438.

Zennaro, M.-C., Boulkroun, S. and Fernandes-Rosa, F. L. (2020) 'Pathogenesis and treatment of primary aldosteronism', *Nature Reviews Endocrinology*. Springer US, 16(10), pp. 578–589. doi: 10.1038/s41574-020-0382-4.

Zhang, J. *et al.* (2022) 'Detrimental or beneficial: Role of endothelial ENaC in vascular function', *Journal of Cellular Physiology*, 237(1), pp. 29–48. doi: 10.1002/jcp.30505.

Zheng, X. *et al.* (2013) 'Arachidonic acid-induced dilation in human coronary arterioles: convergence of signaling mechanisms on endothelial TRPV4-mediated Ca<sup>2+</sup> entry', *Journal of the American Heart Association*, 2(3), p. e000080. doi: 10.1161/JAHA.113.000080.

Zuccolo, E. *et al.* (2017) 'Acetylcholine induces intracellular Ca<sup>2+</sup> oscillations and nitric oxide release in mouse brain endothelial cells', *Cell Calcium*. Elsevier Ltd, 66, pp. 33–47. doi: 10.1016/j.ceca.2017.06.003.

Zuccolo, E. *et al.* (2019) 'Muscarinic M5 receptors trigger acetylcholine-induced Ca<sup>2+</sup> signals and nitric oxide release in human brain microvascular endothelial cells', *Journal of Cellular Physiology*, 234(4), pp. 4540–4562. doi: 10.1002/jcp.27234.

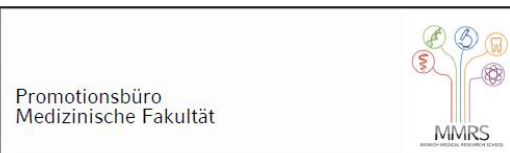
## **Acknowledgements**

I am deeply indebted to Professor Dr. med. Martin Reincke for allowing me to perform this thesis at his institute. It has been a great scientific and intercultural experience for me which has shaped me forever.

I would also like to thank Michaela Höhne for her continuous support with the lab techniques. Your patience and warm heart make working with you a real pleasure.

Finally, I want to thank my supervisor, Dr. med. Holger Schneider, for helping me to put the results into context and providing guidance through the scientific jungle.

## Affidavit



### Affidavit

Meng, Yao

Surname, first name

Street

Zip code, town, country

I hereby declare, that the submitted thesis entitled:

**Aldosterone-induced changes in endothelial function: The epoxyeicosatrienoic acid pathway in aldosterone excess and receptor transactivation by co-stimulation with glucocorticoids.**

is my own work. I have only used the sources indicated and have not made unauthorised use of services of a third party. Where the work of others has been quoted or reproduced, the source is always given.

I further declare that the submitted thesis or parts thereof have not been presented as part of an examination degree to any other university.

Munich, 01.04.2022

Meng Yao

place, date

Signature doctoral candidate

## List of publications

Results of part A have been submitted for publication. The manuscript is currently undergoing a revision. Also, the data were made publicly available on a pre-print server (<https://doi.org/10.1101/2021.02.04.429624>):

Brunnenkant L\*, Meng Y\*, Sun J, Gonzalez Marques J, Koletzko B, Mederos y Schnitzler M, Gudermann T, Williams TA, Beuschlein F, Heinrich DA, Adolf C, Reincke M, Schneider H: The epoxyeicosatrienoic pathway is intact in endothelial and smooth muscle cells exposed to aldosterone excess; bioRxiv; 2021 (\*, shared first authorship)

A manuscript summarizing the results of part B is in preparation.

### Congress contributions

Poster presentation at the virtual European Congress of Endocrinology (ECE) 2020: Intact endothelial epoxyeicosatrienoic acid pathway in primary aldosteronism – the route to new treatment strategies?

Oral presentation at the virtual congress of the European Society of Hypertension (ESH)/International Society of Hypertension (ISH) joint meeting 2021: Gluco- and mineralocorticoids synergistically downregulate BK<sub>Ca</sub> channel transcription in vascular smooth muscle cells but do not affect the epoxyeicosatrienoic acid pathway.